Ren *et al. Biochar* (2026) 8:95
https://doi.org/10.1007/s42773-026-00609-9

Biochar

ORIGINAL RESEARCH Open Access

Global evaluation of a new biochar model for supporting climate-smart agriculture

Wei Ren[1*], Yogesh Kumar[1] and Yawen Huang[1,2]

Abstract

Biochar is a promising climate-smart agriculture (CSA) solution to sustainably support food security while mitigating the adverse impacts of climate change on agroecosystems. Yet, its effectiveness across diverse environments is not well quantified. We developed a process-based biochar model and used it to evaluate biochar's impacts on agroecosystem production and the dynamics of soil biogeochemical cycles (e.g., key CSA indicators such as crop yield, soil organic carbon (SOC), and greenhouse gas (GHG) emissions) across 48 globally distributed field experiment sites. The biochar model was calibrated and evaluated in maize, wheat, and soybean cropping systems, with an average root mean square error of 1878.9 kg ha^{-1} ($R^2 = 0.78$) for crop yield, 4129.3 kg C ha^{-1} ($R^2 = 0.72$) for SOC, and 1995.7 kg CO_2 ha^{-1} ($R^2 = 0.91$) for GHG emissions. The model accuracy varied across environments, with yield predictions performing better in tropical ($R^2 = 0.90$) and temperate ($R^2 = 0.81$) zones and on medium-textured soils ($R^2 = 0.87$), but declining in arid regions ($R^2 = 0.55$) and on coarse soils ($R^2 = 0.65$). Simulation accuracy of SOC and CO_2 was higher in maize than in soybean systems. Biochar application rates also influenced model performance, with medium rates best for crop yield and high rates optimal for SOC and CO_2 emissions. These results highlight the need for robust modeling tools to optimize biochar application across diverse soil and climate conditions. These tools can be important for stakeholders, from farmers to policymakers, and can help refine biochar management strategies and advance global goals of sustainable intensification and net-zero agricultural systems.

Highlights

- A process-based biochar model was developed and calibrated using observational data from 48 global field studies.
- Model's performance was evaluated across a range of climate conditions, soil types, cropping systems, and biochar application rates.
- The model serves as a robust tool for optimizing site-specific biochar application and advancing climate-smart agriculture.

Keywords Biochar modeling, Climate-smart agriculture, DLEM-Ag-Biochar, Crop yield, Soil organic carbon (SOC), Greenhouse gases (GHGs)

*Correspondence:
Wei Ren
wei.ren@uconn.edu
Full list of author information is available at the end of the article

Springer

Graphical Abstract

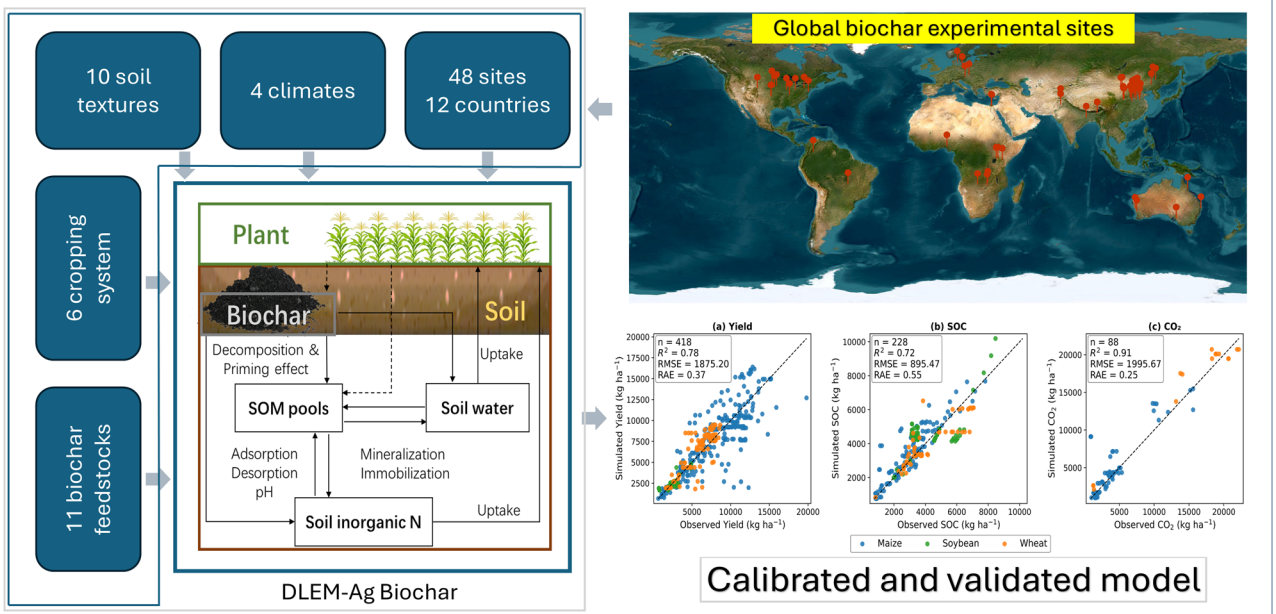

1 Introduction

Biochar, a carbon-rich material produced by the pyrolysis of biomass, is a promising tool for mitigating the impacts of climate change and supporting sustainable agriculture (Laird et al. 2010; Woolf et al. 2010). Owing to its high porosity and nutrient retention capacity, biochar can improve soil health, sequester carbon, and reduce greenhouse gas (GHG) emissions (Atkinson et al. 2010; Lehmann et al. 2011). Recent syntheses indicate that biochar functions as a climate-smart agriculture (CSA) practice that can raise crop yield, enhance soil resilience, and mitigate GHGs, although responses vary across different environments (Jeffery et al. 2011; Wang et al. 2019; Lehmann et al. 2021; Huang et al. 2023; Shrestha et al. 2023; Kaur et al. 2023; Schmidt et al. 2021). Achieving broad and equitable adoption will therefore require a deeper understanding of biochar effects across climate zones, soil types, and cropping systems.

Biochar influences agricultural systems through coupled biogeochemical, hydrologic, and plant processes. Biochar's primary benefit is long-term carbon sequestration in soils (Lehmann et al. 2006; Wang et al. 2016). This benefit can be moderated by priming effects, in which biochar alters the decomposition of native soil organic matter (Kuzyakov and Gavrichkova 2010). The porous structure and reactive surfaces can increase nutrient retention, especially nitrogen, which helps in reducing nitrate leaching and suppressing nitrous oxide emissions (Lehmann et al. 2011). Enhancing soil carbon storage, water holding capacity, and nutrient availability can result in higher crop yields, although the magnitude depends on feedstock, pyrolysis conditions, soil properties, climate, and management (Jeffery et al. 2011; Joseph et al. 2010; Ippolito et al. 2020; Pulcher et al. 2022).

Several studies have advanced the understanding of biochar degradation and its impacts on soil biogeochemical dynamics. Laboratory and greenhouse experiments have provided mechanistic insight into biochar–soil interactions and biochar aging processes (Huang et al. 2023), while short-term field trials have documented immediate impacts during the first years after application (Ventura et al. 2015). However, laboratory studies cannot capture the heterogeneity and variability of natural systems, and short trials may overestimate stability or underestimate priming under a changing climate and management. Long-term field studies, which are essential for assessing real-world outcomes, remain limited in number, sites, and conditions (Jones et al. 2012; Gurwick et al. 2013). Consequently, essential uncertainties persist regarding the durability of effects on productivity, nutrient cycling, and GHG budgets (Archontoulis et al. 2016; Huang et al. 2023).

Models provide a powerful tool for synthesizing diverse evidence and exploring outcomes across different scales and scenarios. Empirical models can predict yield responses but are constrained to the conditions

represented in the underlying training data (Crane-Droesch et al. 2013). Laboratory-derived kinetic models, such as two-pool decay frameworks for labile and recalcitrant carbon, help clarify fundamental processes (Zimmerman et al. 2011), yet the application of results from controlled labs to heterogeneous field and regional contexts remains challenging (Lehmann et al. 2021). Process-based models address this gap by explicitly representing feedback among biochar, soil properties, plants, and climate, which enables evaluation of long-term effects on soil carbon, nutrient cycling, and GHGs, and allows scenario analyses across different management and environmental conditions (Lehmann et al. 2011; Woolf et al. 2010).

Several established process-based models have now developed biochar-specific modules, such as APSIM, DNDC, EPIC, RothC, and the more recent MIMICS-BC (Smith et al. 2008; Wang et al. 2016; Han et al. 2024). RothC and DNDC incorporate biochar decomposition kinetics and interactions with soil organic matter, supporting projections of long-term dynamics (Wang et al. 2016). APSIM and EPIC have been used to simulate biochar impacts on yields and nutrient cycling across management and climate scenarios (Archontoulis et al. 2016). MIMICS-BC advances the field by explicitly representing microbial and physicochemical processes that govern biochar turnover and its influence on soil carbon pools (Han et al. 2024). These efforts demonstrate persistent biochar effects over decadal to centennial scales and across climatic regimes (Ameloot et al. 2013; Zhang et al. 2012b). Nonetheless, global-scale applications remain limited, necessitating broader calibration and validation across diverse crop types, soils, and climates (Smith 2016; Han et al. 2024). Another limitation is the focus on single outcome, such as carbon sequestration or yield, rather than a holistic evaluation that combines productivity, soil carbon, and GHG mitigation within a unified CSA framework (Woolf et al. 2010). Ultimately, model accuracy depends on robust parameterization and careful evaluation against diverse field observations. This critical step, however, is constrained by the scarcity of long-term datasets (Gurwick et al. 2013; Huang et al. 2023; Smith 2004).

In this study, we implemented a newly developed biochar module within the DLEM-Ag framework to evaluate biochar effects on crop yield, soil organic carbon (SOC), and GHG emissions across global field sites that span diverse soils, climates, and cropping systems. To ensure consistent crop parameterization and sufficient sample support for calibration and evaluation, we restricted the analysis to maize, soybean, and wheat systems, including monocultures and rotations among these crops. These crops represent dominant global cereal and oilseed production and are widely represented in field datasets, providing a comparable basis for cross-site model benchmarking. By coupling biochar processes with soil, plant, and atmospheric interactions, we provide a comprehensive assessment of biochar as a CSA practice. The objectives are to: (i) introduce the new biochar module in DLEM-Ag, (ii) calibrate and evaluate model performance for crop and soil responses to biochar across contrasting systems and environments, and (iii) assess model sensitivity to key input parameters that influence simulated biochar impacts.

2 Material and methods

2.1 Model description

Dynamic Land Ecosystem Model-Agriculture (DLEM-Ag) simulates crop growth and carbon, water, and nitrogen dynamics in agricultural ecosystems affected by multiple environmental and management factors at a daily time step. It has been extensively applied to study crop production, cropland SOC, and GHG emissions from global agroecosystems (Ren et al. 2011, 2012, 2016, 2020; Ren 2019; Tian et al. 2012; Huang et al. 2020, 2021, 2022, 2024; Wang et al., 2025).

The DLEM-Ag consists of six SOC pools (i.e., three microbial pools, two slow organic carbon pools, and one dissolved organic carbon pool), plus two woody debris pools (above- and belowground woody debris), and four litter pools (above- and belowground, easy and resistant to decomposition). The sizes of each pool and the carbon fluxes transferred between pools determine the sources and sinks of soil organic and inorganic carbon. Generally, all carbon inputs, including crop residues and roots, are allocated to litter pools based on the carbon-to-nitrogen ratio. Then, carbon fluxes are transferred between pools through biological decomposition, physical adsorption and desorption, surface runoff, and leaching. The decomposition rate of each pool is estimated using a first-order algorithm (Parton et al. 1994) that is influenced by soil temperature, water content, nutrient availability, and soil texture. Details can be found in previous studies (e.g., Banger et al. 2015; Ren et al. 2012, 2020; Tian et al. 2015).

2.2 Biochar module

In this study, we improved the DLEM-Ag model by incorporating a biochar sub-module (DLEM-Ag-Biochar) to specifically examine the effects of biochar on agroecosystems. Biochar was introduced into the DLEM-Ag model as a new type of organic input. The two-pool model was used to represent biochar, i.e., a labile carbon pool and a recalcitrant carbon pool. The biochar sub-module starts by considering the decomposition of biochar and the associated carbon flows (Fig. 1). Due to the often alkaline, porous structure of biochar and its carbon stability, the

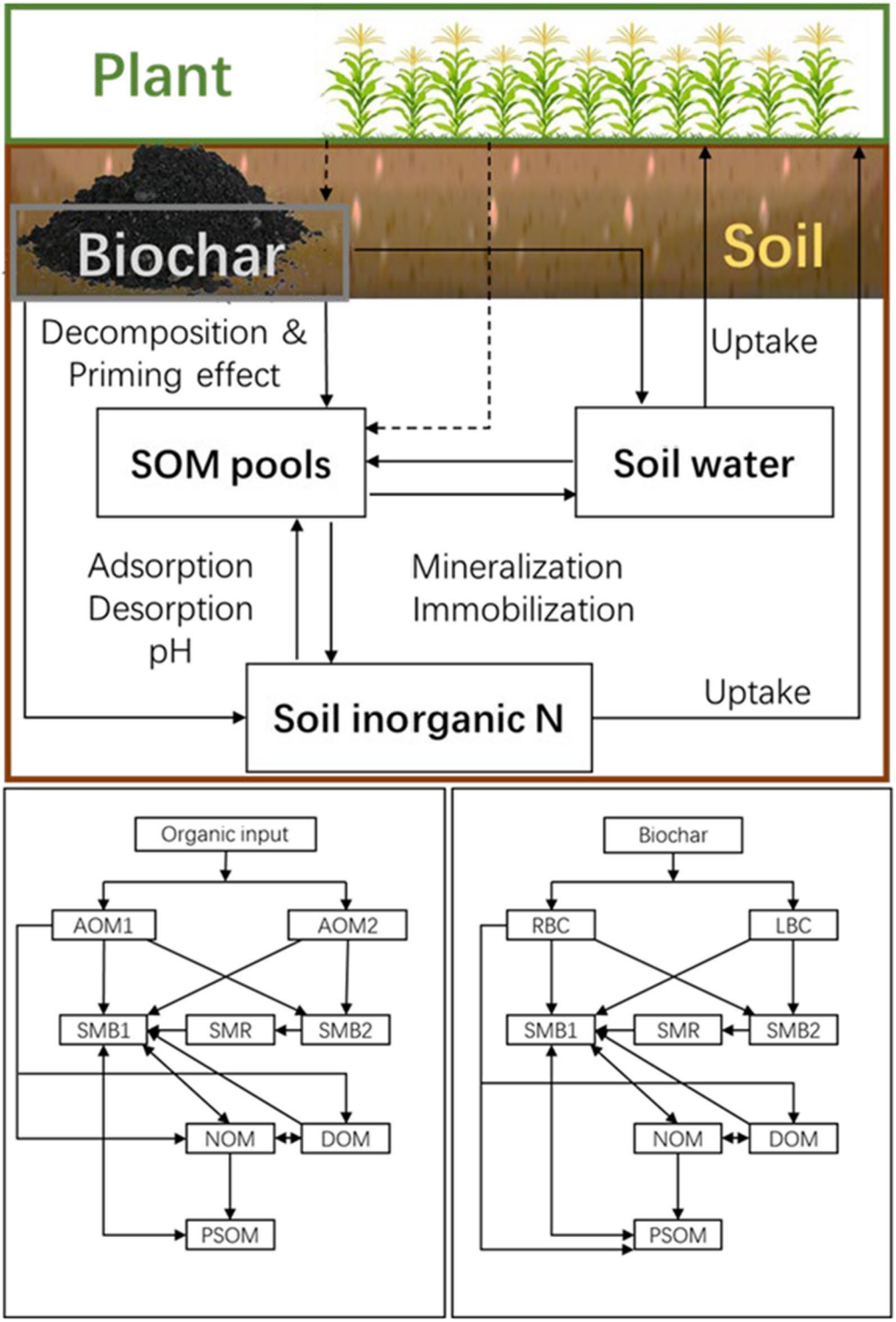

Fig. 1 The flowchart of biochar carbon in the soil

sub-module also considers biochar's effect on soil physicochemical properties and the priming effect on soil native organic carbon, and therefore the biogeochemical processes embedded in DLEM-Ag. More details are given below.

2.2.1 Biochar decomposition and the associated carbon fluxes

Biochar contains both fast- and slow-mineralizing components with vastly different turnover rates (Lehmann et al. 2021). Therefore, the development of the biochar module begins by introducing two biochar carbon pools: one labile (blc) and one recalcitrant (brc). The daily turnover of biochar is calculated as:

$$\Delta C_{bc} = bc \times (1 - f_{loss}) \times f_c \times \left(f_{labile} \times k_1 + (1 - f_{labile}) \times k_2\right) \quad (1)$$

$$k_1 = k_{blc}/365 \times f(T) \times f(W) \times f(N) \quad (2)$$

$$k_2 = k_{brc}/365 \times f(T) \times f(W) \times f(N) \quad (3)$$

where ΔC_{bc} is the amount of biochar carbon that decomposes every day (kg C ha^{-1} day^{-1}); bc is the amount of biochar applied (t ha^{-1}); f_{loss} is the fraction of biochar that is lost during application (0–1); f_c is biochar's carbon fraction (0–1); f_{labile} is biochar's labile carbon fraction (0–1); k_{blc} and k_{brc} are the mean turnover rate, for the labile and recalcitrant biochar pools ($year^{-1}$), respectively; and $f(T)$, $f(W)$, and $f(N)$ are the soil temperature, moisture, and nitrogen modifiers (0–1), which are similar to those used by DLEM-Ag for other SOC pools.

The fate of decomposed biochar includes carbon emitted to the atmosphere and carbon transferred to other SOC pools, including microbial carbon and passive SOC pools. The carbon fluxes from the labile biochar carbon are calculated as:

$$rh_{blc} = frh_{blc} \times \Delta C_{blc} \quad (4)$$

$$C_{blc\_SMB1} = (1 - frh_{blc}) \times f_{blc\_SMB1} \times \Delta C_{blc} \quad (5)$$

$$C_{blc\_SMB2} = (1 - frh_{blc}) \times f_{blc\_SMB2} \times \Delta C_{blc} \quad (6)$$

The carbon fluxes from the recalcitrant biochar carbon are calculated as:

$$rh_{brc} = 0.3 \times f\left(lignin\right) \times \Delta C_{brc} + frh_{brc} \times (1 - f\left(lignin\right)) \times \Delta C_{brc} \quad (7)$$

$$C_{brc\_PSOM} = 0.7 \times f\left(lignin\right) \times \Delta C_{blc} \quad (8)$$

$$C_{brc\_SMB1} = (1 - frh_{brc}) \times (1 - f(lignin) \times f_{brc\_SMB1} \times \Delta C_{blc} \quad (9)$$

$$C_{brc\_SMB2} = (1 - frh_{brc}) \times (1 - f(lignin) \times f_{brc\_SMB2} \times \Delta C_{blc} \quad (10)$$

where rh_{blc} and rh_{brc} are the daily respiration loss of biochar carbon; C_{i_j} is the daily carbon flux from pool i to pool j; ΔC_{blc} and ΔC_{brc} are the daily decomposed biochar carbon; f_{i_j} is the fraction of the decomposed carbon pool i to pool j; frh_{blc} and frh_{brc} represent the respiration fraction of each biochar carbon pool; $f(lignin)$ is the lignin factor, set to 0.3.

2.2.2 Effects on native organic carbon decomposition

Biochar alters native SOC mineralization through priming effects that can be positive, negative, or neutral. Biochar-induced priming effects are calculated in a similar manner following the functions from Archontoulis et al. (2016). The positive priming effect on the litter pool (AOM) is calculated as:

$$k_{AOM\_bc} = k_{AOM} \times (1 + P_{AOM} \times bc') \quad (11)$$

where k_{AOM_bc} is the new dynamic decomposition rate for each of the four DLEM-Ag litter pools (AOM); k_{AOM} is the original decomposition rate of each litter pool; bc' is the biochar carbon (g C m^{-2}) remaining in the soil; P_{AOM} is the positive priming coefficient (m^2 g^{-1} C). The adverse priming effects on AOM are simulated by increasing carbon flux from AOM to the more stable native organic matter (NOM) pool and simultaneously decreasing the respired fraction of AOM:

$$f\left(lignin\_bc\right) = f\left(lignin\right) \times (1 + P_e \times BC), (P_e > 0) \quad (12)$$

$$frh_{AOM\_bc} = frh_{AOM} \times \left(1 + P_f \times BC\right), (P_f < 0) \quad (13)$$

where $f\left(lignin\_bc\right)$ is the modified $f\left(lignin\right)$ parameter that determines the amount of carbon retained in the system (0–1); frh_{AOM_bc} is the modified frh_{AOM} parameter that determines the carbon flux from AOM to other soil carbon pools; P_e and P_f are the negative priming coefficients (m^2 g^{-1} C). Biochar-induced positive and negative priming effects on other SOC pools (i.e., SMB1, SMB2, SMR, NOM, and POM) are calculated in a similar way.

2.2.3 Effects on soil nitrogen mineralization/immobilization

The DLEM-Ag-Biochar first calculates a nitrogen flux based on the biochar's C:N ratio, then adjusts it to account for mineralization and immobilization. Nitrogen mineralization or immobilization depends on whether nitrogen release from biochar decomposition outweighs

nitrogen retention in microbial biomass and stabilized organic matter. The nitrogen flux from the biochar pool (*blc* and *brc*) is:

$$N_{blc\_SMB1} = f_{blc\_SMB1} N_{blc} k_1 \tag{14}$$

$$N_{blc\_SMB2} = f_{blc\_SMB2} N_{blc} k_1 \tag{15}$$

$$N_{brc\_PSOM} = f(lignin) N_{brc} k_2 \tag{16}$$

$$N_{brc\_SMB1} = (1 - f(lignin)) f_{brc\_SMB1} N_{brc} k_2 \tag{17}$$

$$N_{brc\_SMB2} = (1 - f(lignin)) f_{brc\_SMB2} N_{brc} k_2 \tag{18}$$

where N_i is the nitrogen content of pool i and N_{i_j} is the daily nitrogen flux from pool i to pool j. The C:N ratios of fluxes are not always equal to the specific C:N ratio of the destination pool. In transfer processes, if the ratio of carbon flux to nitrogen flux is less than the specific value ($\frac{C_{i\_j}}{N_{i\_j}} < CN_j$), extra organic nitrogen is mineralized and added to the inorganic nitrogen pool as ammonia. The mineralized nitrogen of pool i is:

$$Nmin_i = N_{i\_j} - C_{i\_j}/CN_j \tag{19}$$

The nitrogen flux to the destination pool is:

$$\Delta N_j = C_{i\_j}/CN_j \tag{20}$$

Ammonia pool is updated as:

$$\Delta av_{NH4} = Nmin_i \tag{21}$$

If the ratio of carbon flux to nitrogen flux is higher than the specific value ($\frac{C_{i\_j}}{N_{i\_j}} > CN_j$), the organic pool immobilizes inorganic nitrogen, decreasing the C:N ratio to a specific value. The immobilization rate ($Nimm_i$) is:

$$Nimm_i = \min(\frac{C_{i\_j}}{CN_j} - N_{i\_j}, avn) \tag{22}$$

where avn is the soil available inorganic nitrogen. The changes in the destination nitrogen pool is:

$$\Delta n_j = N_{i\_j} + Nimm_i \tag{23}$$

Given microbial communities' general preference for ammonia (NH_4^+) over nitrate (NO_3^-), the model quantifies immobilized nitrogen as:

$$Nimm_{i,NH4} = Nimm_i \times \frac{av_{NH4}/avn}{\beta + (1-\beta) av_{NH4}/avn} \tag{24}$$

$$Nimm_{i,NO3} = Nimm_i - Nimm_{i,NH4} \tag{25}$$

where β is a constant (0.5). And the changes in ammonia and nitrate pools are updated as:

$$\Delta av_{NH4} = -Nimm_{i,NH4} \tag{26}$$

$$\Delta av_{NO3} = -Nimm_{i,NO3} \tag{27}$$

2.2.4 Effects on soil cation exchange capacity and pH

Biochar generally has a high cation exchange capacity (CEC) due to its oxidized functional groups and large surface area. The DLEM-Ag-Biochar includes the mechanistic representations of soil CEC dynamics and biochar-CEC interactions. When soil CEC data are not available, the model estimates initial soil CEC based on SOC, clay content, and soil order following Seybold and Grossman (2006):

$$CEC_{soil} = f(\%clay, SOC, order) \tag{28}$$

The composite CEC of the soil-biochar mixture is determined through:

$$CEC_{mix} = \frac{CEC_{soil} \times M_{soil} + M_{bc} \times CEC_{bc}}{M_{soil} + M_{bc}} \tag{29}$$

where CEC_{soil}, CEC_{bc}, and CEC_{mix} are the CEC of soil, biochar, and soil-biochar mixture ($cmol_c\ kg^{-1}$), respectively; M_{soil} and M_{bc} are the mass of soil and biochar ($kg\ C\ ha^{-1}$), respectively.

The typical alkaline property of biochar, arising from its inorganic ash constituents and surface functional groups, influences soil pH dynamics. Based on the proportionality between soil buffering capacity and CEC (Nelson and Su 2010), we employed an S-shaped response curve to quantify biochar-mediated pH changes:

$$pH_{mix} = pH_{soil} + \frac{M_{bc} \times BC_{lv}}{(M_{soil} + M_{bc}) \times CEC_{bc}} \times \frac{(pH_u - pH_{soil}) \times (pH_{soil} - pH_l) \times c_0}{(pH_u - pH_l)} \tag{30}$$

where pH_{soil}, pH_{bc}, and pH_{mix} are the pH of soil, biochar, and soil-biochar mixture; BC_{lv} is the lime value of biochar ($cmol_c\ kg^{-1}$), representing the amount of acid that the biochar can neutralize; pH_u and pH_l are the upper and lower limit of soil pH (set at 8.3 and 3.5, respectively), and c_0 is a fitted constant that adjusts soil buffer capacity (set at 10). As noted by Archontoulis et al. (2016), this representation of biochar's effect on CEC and pH is a simplified, empirically grounded approach to

account for the aging effect, without explicitly identifying the specific mechanisms.

2.2.5 Effects on ammonia adsorption/desorption

The high CEC of biochar promotes NH_4^+ adsorption. We quantified biochar-induced NH_4^+ adsorption using the Langmuir model following Gai et al. (2014):

$$NH_{4ads} = av_{NH4} \times \frac{k_{ads} \times (CEC_{mix}/CEC_{soil})}{1 + k_{ads} \times (CEC_{mix}/CEC_{soil})} \quad (31)$$

where NH_{4ads} is the adsorbed NH_4^+ from the soil solution, and k_{ads} is the user-defined adsorption capacity. Based on the equilibrium assumption that adsorbed NH_4^+ will gradually re-enter the soil solution, we model desorption as the reverse of the adsorption process:

$$NH_{4des} = av_{NH4} \times \frac{k_{des} \times (CEC_{mix}/CEC_{soil})}{1 + k_{des} \times (CEC_{mix}/CEC_{soil})} \quad (32)$$

where NH_{4des} is the NH_4^+ desorbed to the soil, and k_{des} is the user-defined deposition coefficient.

2.2.6 Effects on soil water

The effect of biochar on soil water retention parameters in DLEM-Ag (wilting point, field capacity, and saturation point) is modeled according to Archontoulis et al. (2016). Studies indicate that while the wilting point remains largely unaffected by biochar addition, both field capacity and saturation point exhibit modifications dependent on initial SOC content and biochar properties. The effect of biochar on field capacity and saturation point are estimated as follows:

$$\theta_{fc\_BC} = \theta_{fc} \times e^{(-k_{fc} \times SOC)} \quad (33)$$

$$\theta_{sat\_BC} = \theta_{sat} \times e^{(-k_{sat} \times SOC)} \quad (34)$$

where θ_{fc} and θ_{fc_BC} are the soil volumetric water content at field capacity before and after biochar addition, respectively; θ_{sat} and θ_{sat_BC} are the soil volumetric water content at saturation before and after biochar addition, respectively; k_{fc} and k_{sat} are the user-defined parameters.

2.3 Model calibration and evaluation

2.3.1 Observation data collection

We identified 48 global cropland sites from a compiled database of published field experiments (Huang et al. 2023). To ensure consistency for model calibration, sites were selected based on two primary selection criteria: (1) only field experiments with paired biochar and control treatments were included, and (2) cropping systems were restricted to maize, soybean, wheat, or any rotation/combination of these three crops. The final dataset (Table S2) comprises measurements of crop yield, SOC, and GHGs (e.g., CO_2), as well as soil properties, biochar characteristics (e.g., feedstock, pyrolysis temperature, and application rate), and management practices, including tillage, fertilization, and irrigation.

2.3.2 Model driving force data

To drive the DLEM-Ag-Biochar model, four types of site-level datasets were collected and compiled: (1) natural environmental factors including climate conditions, atmospheric CO_2, and nitrogen deposition; (2) topography and soil properties (e.g., pH, bulk density, soil texture, and CEC); (3) cropping system; and (4) agronomic practices (nitrogen fertilization rate, irrigation, tillage, residue treatment, rotation, and phenology). The Harmonized World Soil Database was used if site soil information was unavailable. We used the Open Meteo platform to get site-specific climate conditions. Further details on other auxiliary data are available in previous publications (Huang et al. 2021, 2022; Ren et al. 2020).

2.3.3 Calibration and validation for the biochar model

The DLEM-Ag has been extensively parameterized, calibrated, and validated using field data collected worldwide (e.g., Huang et al. 2020, 2021, 2022; Ren et al. 2012, 2016, 2020; Tian et al. 2010; You et al. 2022; Zhang et al. 2018). A list of newly added biochar parameters related to crop growth, SOC, and GHG emissions for calibration, along with their values in this study, is shown in Table S2. Sensitivity analyses for non-biochar (core DLEM) parameters have been previously published and discussed in detail by Zhang et al. (2018) and You et al. (2022) and are not repeated here. We first ran the model with the default parameters and then calibrated it to obtain optimized, refined parameters that yield a close match between observed and simulated crop yields, SOC, and GHGs. Parameter tuning was executed within a ±20% range of first-estimated values according to the principle in Jamieson et al. (1991). The parameters were set to obtain the minimal bias between the simulated and observed values across all sites. After model calibration, these parameter values were used in the subsequent model validation. After model calibration, these parameter values were used in subsequent simulations. The R^2 (coefficient of determination), RAE (relative absolute error), and RSME (root mean square error) were calculated to evaluate the model performance.

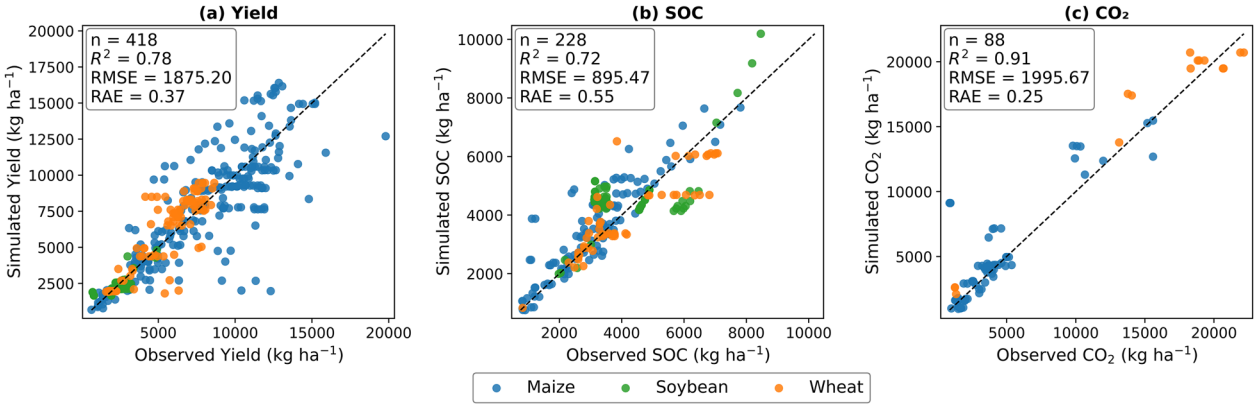

Fig. 2 Overall model performance of the DLEM-Ag-Biochar model in simulating **a** crop yield, **b** soil organic carbon (SOC), and **c** CO_2 emissions across globally distributed biochar field experiment sites

2.3.4 Model implementation

The model simulation began with an equilibration run using long-term average climate data to approach the initial states of the carbon, nitrogen, and water pools before the initiation of the experiment at each site (Huang et al. 2021). The equilibrium state was defined such that the year-to-year changes in carbon, nitrogen, and water pools at the site would be less than 0.1 g C m^{-2}, 0.1 g N m^{-2}, and 0.1 mm H_2O, respectively. In this procedure, we used observed SOC data as the primary constraint, with the model deriving initial values for unmeasured variables (Ren et al. 2020). After the equilibrium run, we conducted a 10-year spin-up using randomly selected climate data to remove abrupt changes caused by the transition from equilibrium to transient mode (Huang et al. 2020). Finally, the model was supplied with time-series input data in the transient mode.

2.4 Parameter sensitivity analysis

We conducted a local, one-at-a-time sensitivity analysis, a perturbation-based approach that varies one parameter at a time around a baseline while holding all others fixed (Hamby 1994; Saltelli et al. 2004). For each biochar-related parameter, we applied −50, −25, 0, +25, and +50 percent changes, re-ran the model for each perturbation, and recorded the resulting changes in target variables (Figs. S1, S2, and S3). The sensitivity of each parameter was evaluated by computing normalized relative changes across perturbation levels (Lenhart et al. 2002; Saltelli et al. 2008). This method reveals the relationship between each parameter and outputs, showing whether responses are linear or nonlinear, and whether there are tipping points where outputs respond drastically to parameter changes (Haghnegahdar and Razavi 2017; Pianosi et al. 2016).

3 Results

3.1 Overall model performance

The DLEM-Ag-Biochar model demonstrated strong performance in simulating crop yield, soil organic carbon (SOC), and CO_2 emissions when compared against field observations (Fig. 1). For crop yield (n = 418), the model achieved a close agreement with observations, yielding an R^2 of 0.78, an RMSE of 1875.20 kg ha^{-1}, and an RAE of 0.37 (Fig. 2a). SOC simulations (n = 228) were also robust, with an R^2 of 0.72, an RMSE of 895.47 kg ha^{-1}, and an RAE of 0.55 (Fig. 2b). The model exhibited the highest accuracy for CO_2 emissions (n = 88), with an R^2 of 0.91, an RMSE of 1995.67 kg ha^{-1}, and an RAE of 0.25 (Fig. 2c).

3.2 Model performance for crop yield

Model performance was evaluated across different crop types, soil textures, climate zones, and biochar application rates (Fig. 3). Parallel boxplots comparing observed and simulated yields, with pairwise significance tests, are shown in Fig. S4a–d. Model performance for crop yield varied by crop type (Fig. 3a), as indicated by distributional contrasts and pairwise tests (Fig. S4a). The highest agreement between simulated and observed yields was achieved for wheat (R^2 = 0.79, RMSE = 1358.14 kg ha^{-1}, RAE = 0.46; n = 107), followed by maize (R^2 = 0.68, RMSE = 2288.04 kg ha^{-1}, RAE = 0.49; n = 239). While soybean yield simulations resulted in the lowest R^2 value (0.58; n = 72), they also exhibited the smallest absolute error (RMSE = 543.70 kg ha^{-1}), a result consistent with the lower absolute magnitude of soybean yields compared to other crops; however, the higher RAE (0.71) indicates larger relative error. When stratified by soil texture (Fig. 3b), model performance was strongest on medium-textured soils, demonstrating the highest

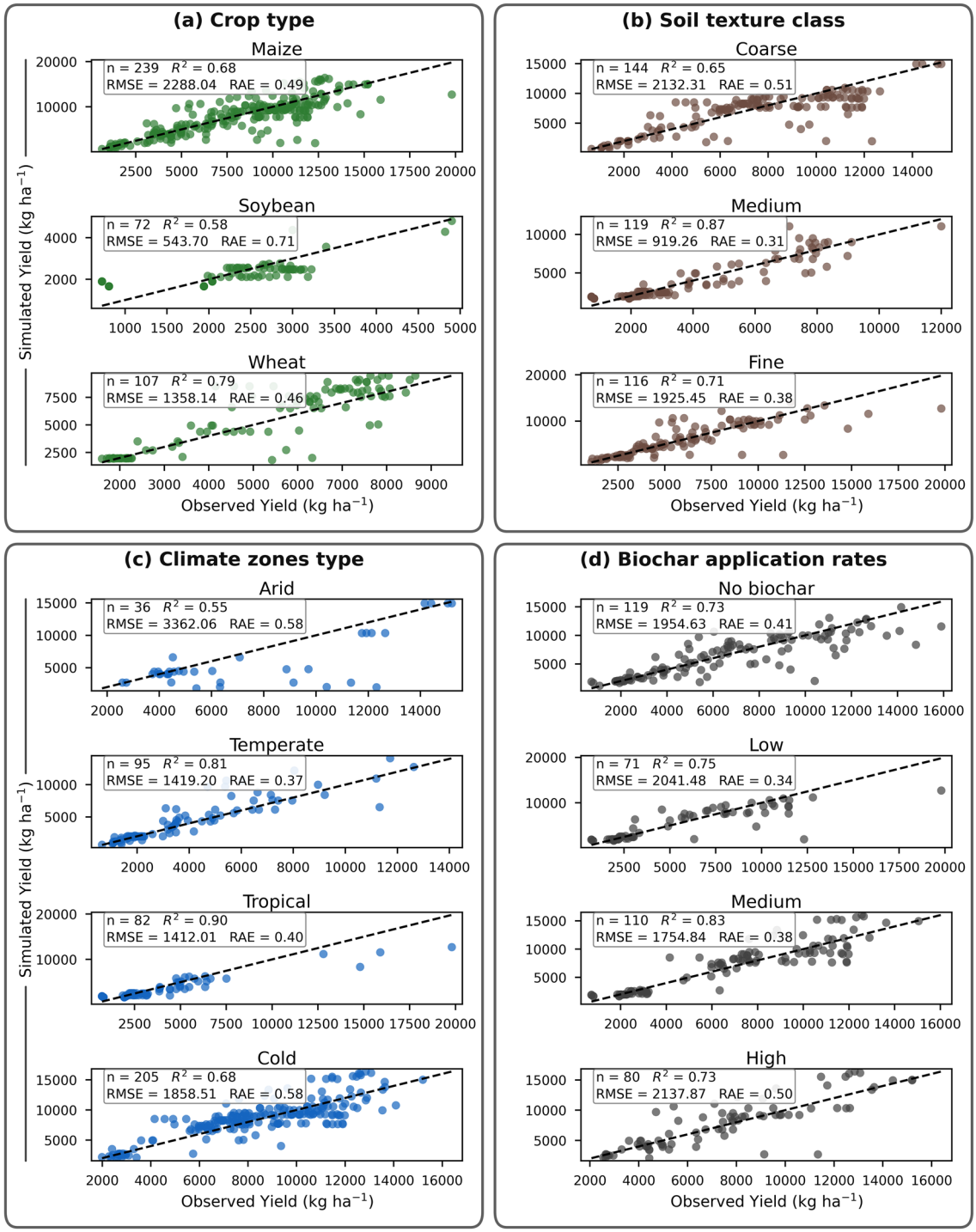

Fig. 3 Model performance in simulating crop yield by crop type (**a**) and soil texture class (**b**) different climate zones (**c**), and under four biochar application rate (**d**) categories: No biochar (0 t ha^{-1}), Low (<5 t ha^{-1}), Medium (5–20 t ha^{-1}), and High (>20 t ha^{-1}) across global field experiment sites. Metrics include the number of observations (n), R^2, RMSE, and RAE

explanatory power ($R^2 = 0.87$) and lowest absolute and relative errors (RMSE = 919.26 kg ha^{-1}, RAE = 0.31; n = 119).

Performance was moderate on fine-textured soils ($R^2 = 0.71$, RMSE = 1925.45 kg ha^{-1}, RAE = 0.38; n = 116) and comparatively lower on coarse-textured soils, which

showed the highest RMSE and RAE values (R^2 = 0.65, RMSE = 2132.31 kg ha^{-1}, RAE = 0.51; n = 144). Observed vs simulated yield distributions by soil texture are shown in Fig. S4b. Model accuracy varied substantially across various climate zones (Fig. 3c). Tropical zones showed the highest agreement (R^2 = 0.90, RMSE = 1412.01 kg ha^{-1}, RAE = 0.40; n = 82), closely followed by temperate zones (R^2 = 0.81, RMSE = 1419.20 kg ha^{-1}, RAE = 0.37; n = 95). Performance was lower in cold (R^2 = 0.68, RMSE = 1858.51 kg ha^{-1}, RAE = 0.58; n = 205) and arid zones, with the latter showing the poorest model fit and largest absolute error (R^2 = 0.55, RMSE = 3362.06 kg ha^{-1}; RAE = 0.58; n = 36). Distributional contrasts across climate zones are shown in Fig. S4c. The model demonstrated robust performance across biochar application rates (Fig. 3d). Medium application rates yielded the strongest correlation (R^2 = 0.83, RMSE = 1754.84 kg ha^{-1}, RAE = 0.38; n = 110). Performance was consistent for no-biochar (R^2 = 0.73, RMSE = 1954.63 kg ha^{-1}, RAE = 0.41; n = 119) and low application treatments (R^2 = 0.75, RMSE = 2041.48 kg ha^{-1}, RAE = 0.34; n = 71). Predictions under high biochar applications maintained the R^2 value of 0.73 (n = 80) but were associated with the highest RMSE (2137.87 kg ha^{-1}) and RAE (0.50) for this category. Category-wise distributions for biochar application rates, with pairwise significance, are shown in Fig. S4d.

3.3 Model performance for soil organic carbon (SOC)

The performance of the biochar model in simulating soil organic carbon (SOC) stocks was evaluated across various conditions (Fig. 4). Parallel boxplots comparing observed and simulated SOC, with pairwise significance tests, are shown in Fig. S5a–d. Model accuracy varied substantially by category. Among crop types (Fig. 4b), SOC simulations were most accurate for maize (R^2 = 0.82, RMSE = 765.77 kg ha^{-1}, RAE = 0.48; n = 116) and wheat (R^2 = 0.77, RMSE = 802.11 kg ha^{-1}, RAE = 0.41; n = 53), while soybean systems showed the poorest performance with the lowest R^2 (0.48) and highest errors (RMSE = 1169.55 kg ha^{-1}, RAE = 0.82; n = 59). Distributional differences by crop type are shown in Fig. S5a. Soil texture significantly influenced model performance (Fig. 4b), with excellent agreement on coarse-textured soils (R^2 = 0.97, RMSE = 488.71 kg ha^{-1}, RAE = 0.15; n = 16) and strong performance on fine-textured soils (R^2 = 0.85, RMSE = 807.68 kg ha^{-1}, RAE = 0.32; n = 78). However, accuracy declined on medium-textured soils, which exhibited the lowest explanatory power (R^2 = 0.35) and highest relative error (RAE = 1.01; n = 107). Observed and simulated SOC distributions by soil texture appear in Fig. S5b. Climate conditions substantially affected model performance (Fig. 4c). The strongest correlations were observed in arid (R^2 = 0.85, RMSE = 838.66 kg ha^{-1}, RAE = 0.38; n = 39) and cold zones (R^2 = 0.83, RMSE = 709.02 kg ha^{-1}, RAE = 0.43; n = 116), while tropical zones showed minimal agreement with observations (R^2 = 0.07, RMSE = 1187.50 kg ha^{-1}, RAE = 1.04; n = 63). Distributional contrasts across climate zones are provided in Fig. S5c. Biochar application rates also influenced model accuracy (Fig. 4d), with the strongest performance under no-biochar conditions (R^2 = 0.85, RMSE = 486.04 kg ha^{-1}, RAE = 0.34; n = 76) and high application rates (R^2 = 0.74, RAE = 0.48; n = 68). Predictive capability declined substantially at low application rates (R^2 = 0.26, RMSE = 985.30 kg ha^{-1}, RAE = 0.98; n = 36), indicating challenges in simulating SOC response to moderate biochar amendments. Biochar application rate-specific SOC distributions and corresponding pairwise tests are summarized in Fig. S5d.

3.4 Model performance for greenhouse gas emissions

The performance of the biochar model in simulating cumulative CO_2 emissions was evaluated across multiple categories (Fig. 5). Detailed distributions of observed versus simulated CO_2 by category, with pairwise tests, are provided in Supplementary Fig. S6a–d. Model accuracy varied substantially across crop types (Fig. 5a), with excellent performance for wheat (R^2 = 0.96, RMSE = 1776.33 kg ha^{-1}, RAE = 0.26; n = 15) and moderate performance for maize (R^2 = 0.74, RMSE = 2037.82 kg ha^{-1}, RAE = 0.48; n = 73). Crop-type contrasts are shown in Fig. S6a. No soybean data were available for validation. Soil texture significantly influenced model performance (Fig. 5b), with fine-textured soils showing the strongest agreement (R^2 = 0.96, RMSE = 1580.86 kg ha^{-1}, RAE = 0.18; n = 39), while both coarse- and medium-textured soils exhibited lower explanatory power (R^2 = 0.70 for both). However, medium-textured soils showed lower absolute error (RMSE = 699.77 kg ha^{-1}) but higher relative error (RAE = 0.62; n = 23) compared to coarse-textured soils (RMSE = 3049.27 kg ha^{-1}, RAE = 0.41; n = 26). Soil-texture contrasts are provided in Fig. S6b. Climate conditions substantially affected model accuracy (Fig. 5c), with exceptional performance in temperate zones (R^2 = 0.98, RMSE = 561.27 kg ha^{-1}, RAE = 0.18; n = 10) and strong performance in cold zones (R^2 = 0.91, RMSE = 2167.40 kg ha^{-1}, RAE = 0.22; n = 66). Model performance declined in tropical zones, which showed moderate R^2 (0.54) but extremely high relative error (RAE = 11.52; n = 4), and arid zones, which exhibited minimal explanatory power (R^2 = 0.12, RAE = 1.05; n = 8). Climate-zone distributions appear in Fig. S6c. Biochar application rates

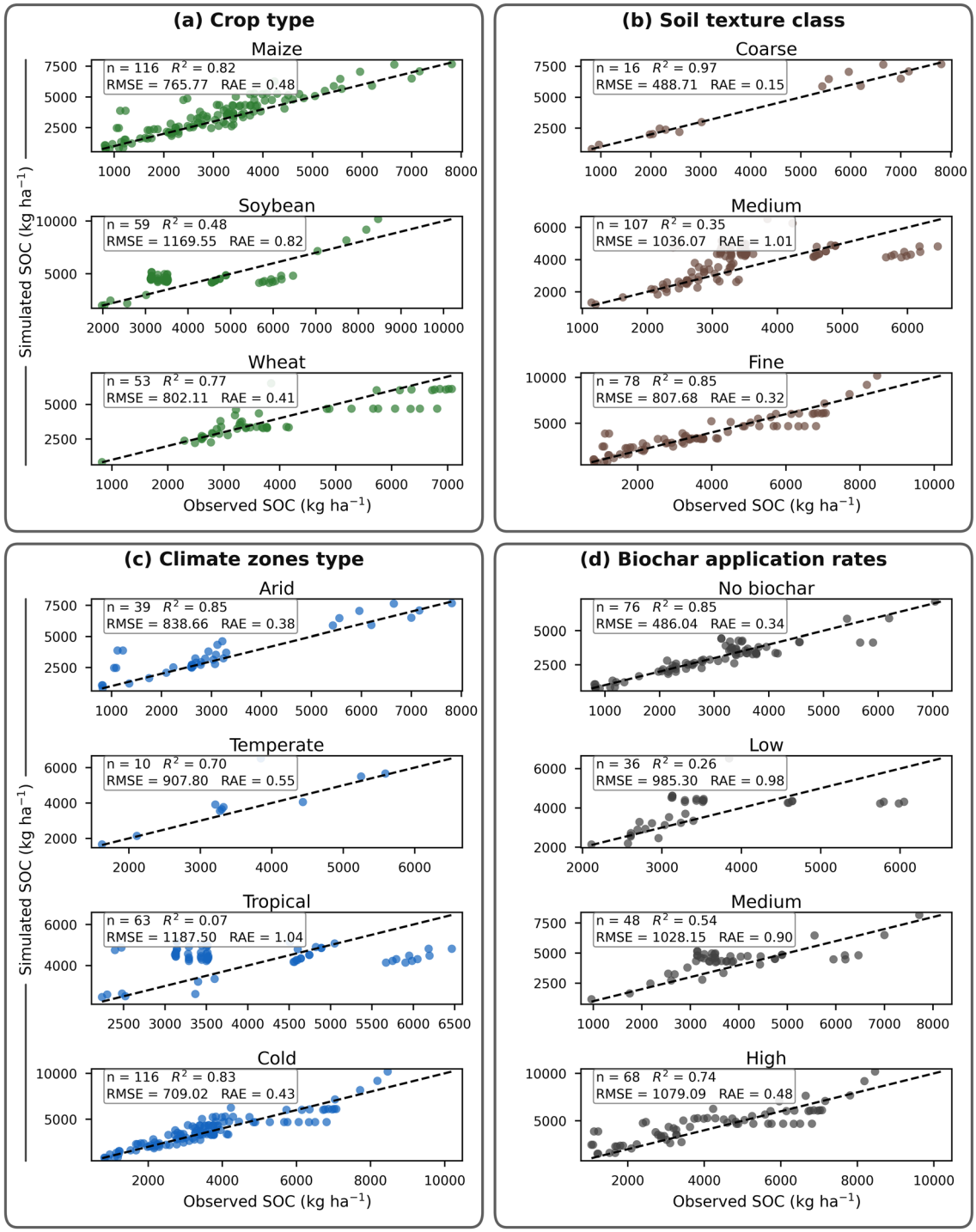

Fig. 4 Model performance in simulating SOC by crop type (**a**) and soil texture class (**b**) different climate zones (**c**), and under four biochar application rate (**d**) categories: No biochar (0 t ha^{-1}), Low (<5 t ha^{-1}), Medium (5–20 t ha^{-1}), and High (>20 t ha^{-1}) across global field experiment sites. Metrics include number of observations (n), R^2, RMSE, and RAE

significantly influenced model performance (Fig. 5d), with the highest accuracy occurring under high application rates (R^2 = 0.99, RMSE = 858.73 kg ha^{-1}, RAE = 0.14; n = 36) and no-biochar conditions (R^2 = 0.95, RMSE = 1321.11 kg ha^{-1}, RAE = 0.20; n = 30). Performance was notably weaker for low application

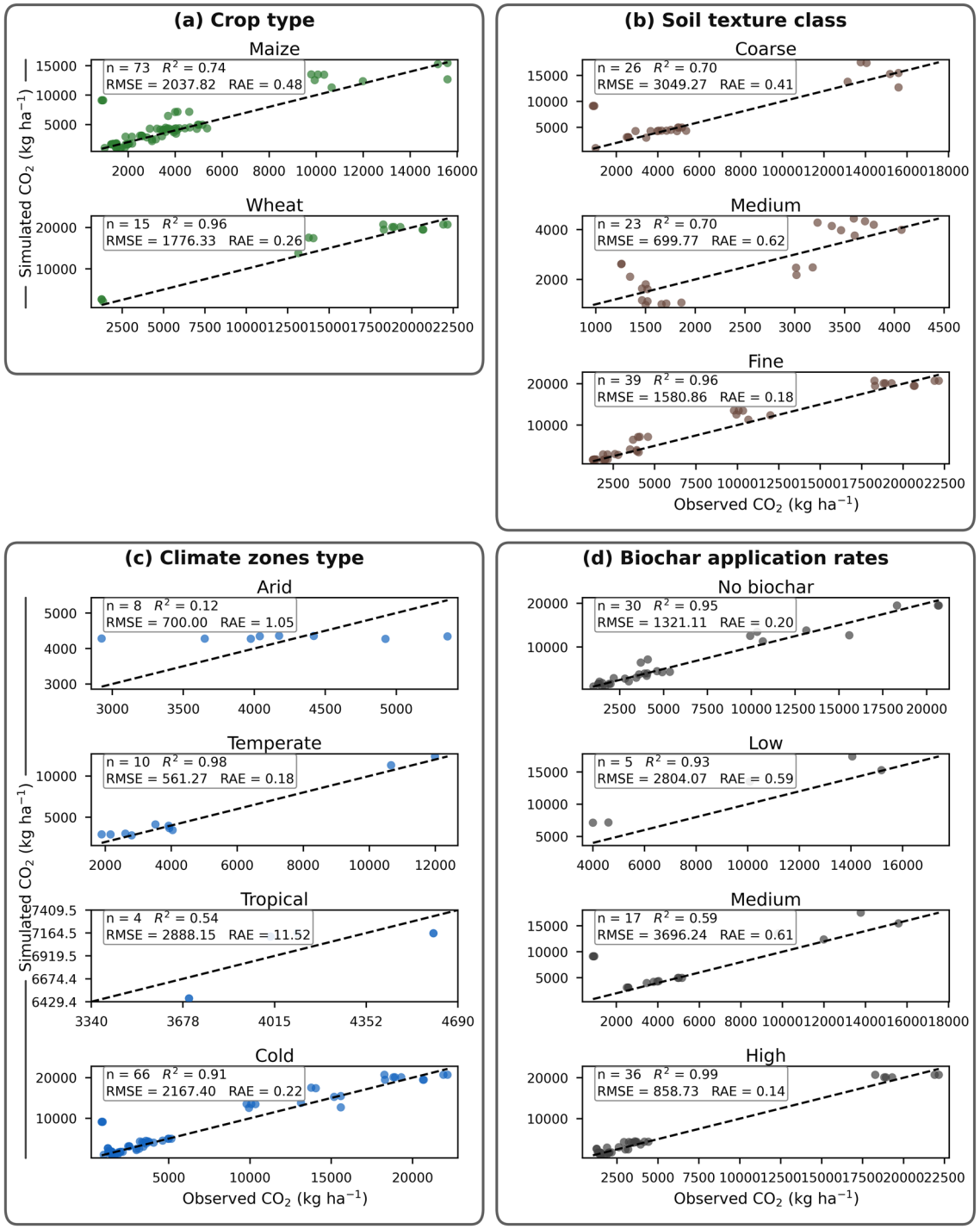

Fig. 5 Model performance in simulating CO_2 by crop type (**a**) and soil texture class (**b**) different climate zones (**c**), and under four biochar application rate (**d**) categories: No biochar (0 t ha^{-1}), Low (<5 t ha^{-1}), Medium (5–20 t ha^{-1}), and High (>20 t ha^{-1}) across global field experiment sites. Metrics include number of observations (n), R^2, RMSE, and RAE

rates (R^2 = 0.93, RMSE = 2804.07 kg ha^{-1}, RAE = 0.59; n = 5) and medium application rates (R^2 = 0.59, RMSE = 3696.24 kg ha^{-1}, RAE = 0.61; n = 17), though the small sample size for low application rates limits the robustness of this assessment. Biochar-rate group

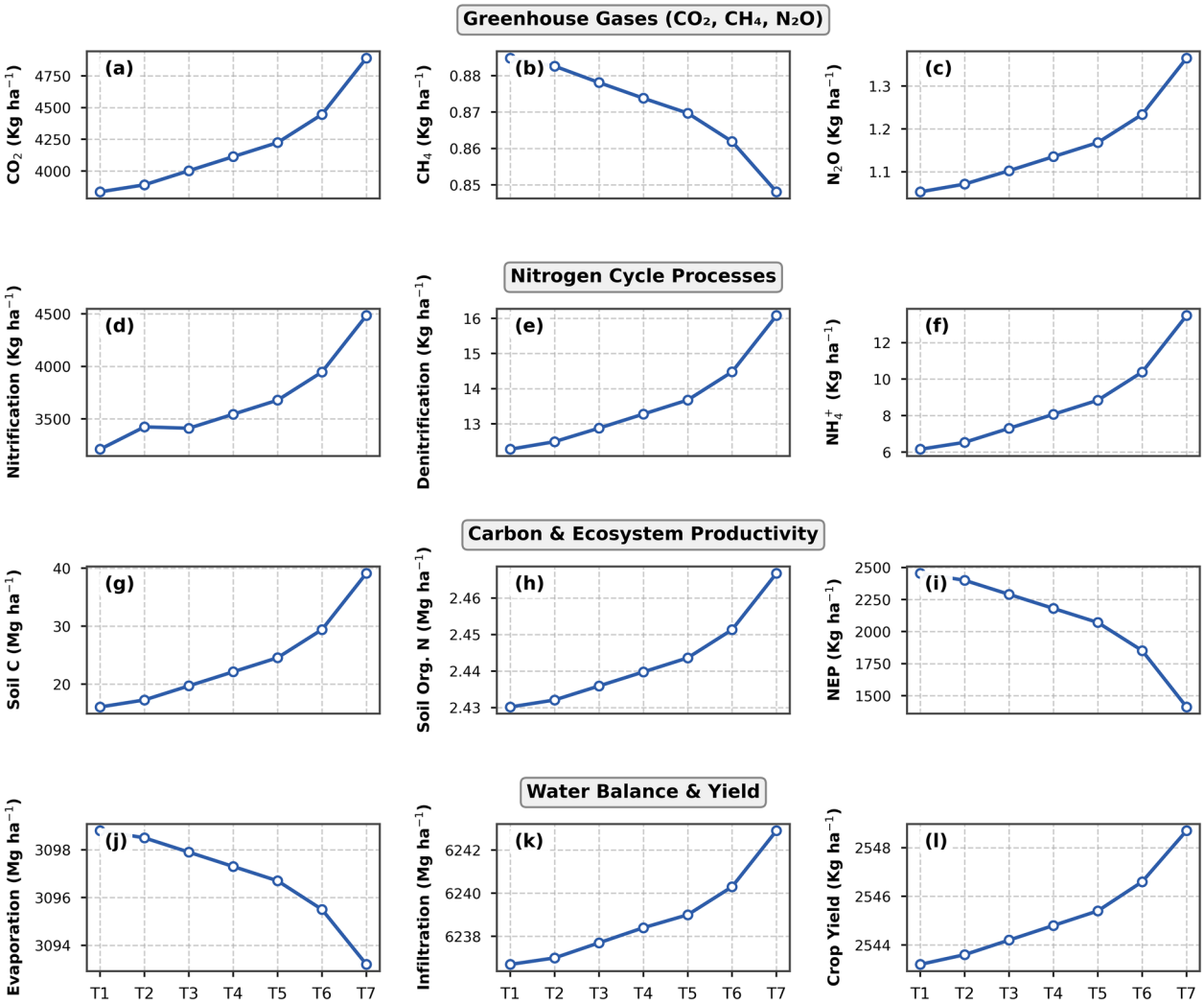

Fig. 6 Sensitivity analysis of the DLEM-Ag-Biochar model for key environmental and biogeochemical processes across varying biochar application rates. Biochar treatments ranged from 2.5 to 50 t ha^{-1}, with T1 to T7 corresponding to 2.5, 5, 10, 15, 20, 30, and 50 t ha^{-1}. Panels show: **a**–**c** Greenhouse gases: cumulative CO_2, CH_4, and N_2O emissions; **d**–**f** Nitrogen cycle processes: nitrification, denitrification, and soil NH_4^+ pool; **g**–**i** Carbon and ecosystem productivity: soil organic carbon, soil organic nitrogen, and net ecosystem production (NEP); **j**–**l** Water balance and yield: cumulative evaporation, infiltration, and grain yield. Evaporation and infiltration are expressed as water-equivalent fluxes

distributions with the corresponding pairwise tests are summarized in Fig. S6d.

3.5 Sensitivity analysis of biochar application rates on environmental variables

A sensitivity analysis was conducted to evaluate the effects of biochar application rates, ranging from 2.5 to 50 t ha^{-1}, on key agronomic and environmental variables (Fig. 6). The results for each measured parameter are presented below. *Greenhouse Gas Emissions:* Carbon dioxide (CO_2) emissions increased substantially with higher application rates, rising from 3836.2 kg ha^{-1} at 2.5 t ha^{-1} to 4889.8 kg ha^{-1} at 50 t ha^{-1}. In contrast, methane (CH_4) emissions exhibited a decreasing trend, declining from 0.8848 kg ha^{-1} at the lowest application rate to 0.8481 kg ha^{-1} at the highest rate. Nitrous oxide (N_2O) emissions demonstrated a pronounced positive response to biochar addition, increasing from 1.0532 kg ha^{-1} to 1.3652 kg ha^{-1} across the treatment range. *Nitrogen Processes:* Nitrification rates increased consistently with application rate, rising from 3210.98 kg ha^{-1} at 2.5 t ha^{-1} to 4483.57 kg ha^{-1} at 50 t ha^{-1}. Similarly, denitrification rates showed a positive correlation, escalating from 12.28 kg ha^{-1} to 16.08 kg ha^{-1}. Soil ammonium (NH_4^+) availability also increased substantially, from 6.15 kg ha^{-1} to 13.49 kg ha^{-1} across the biochar gradient. *Carbon*

and Ecosystem Flux: SOC content increased markedly from 16.06 Mg ha^{-1} to 39.13 Mg ha^{-1} with increasing biochar rates. Conversely, soil organic nitrogen (SON) showed a modest increase, rising from 2.43 Mg ha^{-1} to 2.47 Mg ha^{-1}. The Net Ecosystem Productivity (NEP) exhibited a substantial negative response, decreasing from 2454.6 kg ha^{-1} to 1412.1 kg ha^{-1}. *Water Fluxes and Crop Yield:* The hydrological cycle and agricultural output were also sensitive to biochar amendments. Evaporation showed a slight decreasing trend, declining from 3098.8 Mg ha^{-1} to 3093.2 Mg ha^{-1}. Conversely, infiltration exhibited a positive response, increasing from 6236.7 Mg ha^{-1} to 6242.9 Mg ha^{-1}. Crop yield demonstrated a marginal but consistent increase with biochar application, rising from 2543.2 kg ha^{-1} to 2548.7 kg ha^{-1}.

4 Discussion

4.1 Performance of the DLEM-Ag-Biochar model

The global site-level validation indicates that DLEM-Ag-Biochar reproduces observed crop yield, SOC, and GHG fluxes. Residual bias in simulated yield likely arises from the use of fixed values for key physiological parameters, such as specific leaf area (SLA), maximum nitrogen uptake (MaxNup), and maximum carboxylation rate (Vcmax), despite their known variation over phenology and in response to environmental conditions (You et al. 2022; Danalatos et al. 1994; Tardieu et al. 1999; Lu et al. 2020; Qian et al. 2021; Quebbeman and Ramirez 2016). The seasonal controls on SLA remain insufficiently resolved in current models (Drewniak et al. 2013; You et al. 2022). Spatial patterns of modeled yield broadly align with observations, though discrepancies persist. Across sites, the yield response to biochar application rate was smaller than the responses of SOC and GHGs (Fig. 1). We attribute this attenuation to feedback within the biochar-soil-crop-atmosphere system represented in the model, which can counterbalance process-level effects or render them too small to shift yields. For example, greater soil moisture, which promotes growth, can also enhance nitrate losses via denitrification or leaching, thereby constraining yield gains. Similar behavior has been documented for APSIM's biochar implementation (Archontoulis et al. 2016). Overall, these patterns support our global, multi-crop validation study results and conclusions.

Model performance on crop yield: Model's performance varied across climates, with tropical and temperate zones showing the strongest agreement between modeled and observed yields (Fig. 2). This pattern is consistent with evidence that biochar performs best where moisture and nutrients are abundant, improving soil structure, nutrient retention, and plant growth (Lehmann et al. 2011; Jeffery et al. 2017). In tropical systems, high microbial activity and rapid organic matter turnover intensify nutrient cycling, amplifying gains in fertility and aggregation (Major et al. 2010; Singh et al. 2012). Lower RMSE in these zones indicates that the model captures key pathways linking biochar, moisture, and nutrient availability to yield responses (Kammann et al. 2015; Woolf et al. 2018).

The arid zone showed the weakest correlations and the highest RMSE, indicating constraints that are not fully represented. High temperatures, persistent water deficits, and low organic matter limit biochar effectiveness and complicate simulation of coupled water–nutrient dynamics (Jeffery et al. 2011; Lehmann et al. 2011). Better performance will likely require explicit irrigation scheduling, evapotranspiration feedbacks, and biochar-soil moisture interactions under drought (Kammann et al. 2015; Wang et al. 2021). Although biochar can enhance water retention in dry soils, its effects may vary with application rate and soil properties, reducing predictive accuracy when simplified (Liu et al. 2013; Major et al. 2012). Heterogeneous leaching, sorption, and gas exchange matter, motivating refinements to texture-sensitive parameters and water-balance routines (Spokas et al. 2012; Atkinson et al. 2010). Soil texture further modulated model performance. Fine-textured soils exhibited the highest performance, because greater water-holding capacity and CEC elevate nutrient retention and uptake (Lehmann et al. 2011; Zhang et al. 2012a). Biochar's porosity augments these properties, yielding more consistent responses and smaller errors (Atkinson et al. 2010). Coarse-textured soils with lower moisture storage and higher leaching rates showed moderate performance (Major et al. 2010). Lower R^2 in medium-textured soils suggests the need for additional calibration, including porosity, clay content, and nitrogen cycling pathways (Jeffery et al. 2011). Variation in biochar particle size and composition also influences outcomes and should be represented where data permit (Joseph et al. 2010; Spokas et al. 2012). Model performance also varied with application rate and crop type. At higher rates, accuracy sometimes declined, consistent with reports that excessive biochar raises soil pH and induces nutrient imbalances, particularly for nitrogen, altering rhizosphere activity and uptake (Lehmann et al. 2011, 2020; Jeffery et al. 2017). Performance degradation above ~20 t ha^{-1} highlights the need for balanced strategies that enhance nutrient availability without compromising physicochemical stability (Major et al. 2010; Biederman & Harpole 2013). Among crops, wheat showed the highest predictive accuracy, consistent with benefits from improved moisture retention and nutrient supply (Zhang et al. 2012a, b; Sun et al. 2017). Maize showed moderate performance, reflecting high nutrient demand and the value of pairing biochar with fertility

management (Kammann et al. 2015). Soybean accuracy was lower, plausibly due to reliance on biological nitrogen fixation and a smaller sample size (Rondon et al. 2007; Glaser et al. 2002).

Overall, the results support site-specific biochar strategies that couple application rate, feedstock, and particle size with climate, soil texture, and crop requirements. The model performs well in humid and temperate regions, while water-limited processes constrain applicability in arid systems (Laird et al. 2010; Liu et al. 2013). Priorities include incorporating irrigation dynamics and drought responses, refining hydraulic and nutrient modules across textures, and expanding long-term field validations to reduce parameter uncertainty (Biederman & Harpole 2013; Lehmann et al. 2011). Attention to biochar-microbe interactions can clarify mechanisms linking soil function and yield (Xu et al. 2014). These advances will strengthen the use of biochar within CSA frameworks and improve the generality of models across agroecosystems (Smith 2016; Woolf et al. 2010).

Model performance on SOC: Across cropping systems, biochar rates, and environments, the DLEM-Ag-Biochar model gives reasonable SOC predictions, with varying accuracy (Fig. 3). Higher R^2 values for wheat than for maize indicate that model performance more effectively captures SOC dynamics in wheat systems, consistent with evidence that wheat often sustains steadier SOC accumulation via regular residue inputs and comparatively slower decomposition (Luo et al. 2010; Powlson et al. 2011). Greater variability in maize due to faster residue turnover and shifts in microbial activity, helping explain lower R^2 for maize (Kravchenko et al. 2015; Tiemann et al. 2015). The model performance is notably weaker in soybean systems. A likely reason is the simplified representation of biological nitrogen fixation (BNF). In the current version, BNF is implemented as a static input function and is not dynamically coupled with biochar-induced changes in key soil variables such as pH, nutrient availability, or microbial activity. The model's moderate performance across biochar application rates suggests that, while biochar supports SOC stabilization, explicit representation of microbial interactions, mineral-associated organic matter formation, and management effects remains important (Lehmann et al. 2011; Singh et al. 2012). Climatic contrasts further shape model performance. In temperate regions, where SOC stabilization mechanisms and biochar-induced aggregation are well documented, performance was highest (Woolf et al. 2010; Smith 2016). Tropical sites were challenging, with an R^2 of 0.07, likely reflecting high microbial activity, rapid decomposition, and accelerated biochar aging, which together reduce SOC retention (Cheng et al. 2008; Zimmerman et al. 2011). Cold climates showed moderate performance ($R^2 = 0.55$), suggesting the need to improve parameterization of freeze–thaw dynamics, seasonally reduced microbial activity, and slower decomposition regimes that modulate SOC accrual (Kuzyakov and Gavrichkova 2010; Schimel et al. 2004). These patterns emphasize that biochar-driven SOC responses are conditioned by climate-sensitive processes that must be captured by temperature- and moisture-response functions, as well as by representations of biochar weathering over time.

Soil texture exerted a strong control on predictive accuracy. Medium-textured soils yielded the best performance, consistent with their balanced aeration, water retention, and microbial habitat that favor SOC stabilization (Six et al. 2002; Denef et al. 2001). Coarse soils showed reduced performance ($R^2 = 0.51$), likely reflecting weaker organo-mineral associations, greater leaching, and higher DOC mobility (Hassink 1997; Thangarajan et al. 2013). Fine-textured soils can retain substantial SOC but also exhibit aggregation effects that mediate biochar interactions with native organic matter; capturing these mechanisms would improve predictions (Blanco-Canqui 2017; Laird et al. 2010). Incorporating texture-dependent sorption, pore-size distributions, and water dynamics will better represent SOC stabilization pathways across edaphic contexts. Overall, the results support continued refinement of biochar SOC modeling to account for site-specific climate, texture, and crop effects. Priorities include stronger representation of microbial feedback, priming effects, and age-dependent biochar decomposition processes (Wang et al. 2016; Ameloot et al. 2013), supported by expanded, long-term field datasets for parameterization and validation (Jeffery et al. 2017; Biederman and Harpole 2013). Integrating mechanisms for biochar-mineral associations and microbial-mediated stabilization should further enhance model performance and generality across agroecosystems (Lehmann et al. 2021; Weng et al. 2017).

Model performance on GHG emissions: The substantial R^2 value of 0.96 indicates that the DLEM-Ag-Biochar model performs well in predicting CO_2 emissions following biochar application (Fig. 4). The model's high accuracy aligns with previous studies that have demonstrated the effectiveness of ecosystem models in simulating CO_2 flux dynamics in agricultural landscapes (Smith 2016; Xu et al. 2016). The observed RMSE, while indicating some variance, suggests that minor improvements in model calibration could enhance accuracy, particularly in cases where extreme CO_2 emissions are recorded (Woolf et al. 2010). Factors such as biochar composition, soil microbial activity, and climatic conditions influence CO_2 fluxes, which may contribute to discrepancies between observed

and predicted values (Lehmann et al. 2011; Ameloot et al. 2013). Biochar application has been shown to influence soil respiration and microbial activity, both of which are key regulators of CO_2 emissions. Studies have indicated that biochar can enhance soil carbon sequestration by stabilizing organic matter and reducing microbial decomposition rates, thus lowering overall CO_2 emissions over time (Wang et al. 2016; Kuzyakov and Gavrichkova 2010). However, under certain conditions, biochar-induced priming effects may lead to an initial increase in CO_2 emissions before stabilizing (Zimmerman et al. 2011; Jones et al. 2012). The observed alignment between simulated and measured CO_2 values in this study suggests that the model effectively incorporates these processes, but further refinements may be required to capture short-term fluctuations in CO_2 fluxes more accurately. The slight deviations at higher CO_2 values suggest that the model could benefit from further parameterization, particularly in cases of high organic matter decomposition rates or specific soil conditions that promote enhanced microbial respiration (Jeffery et al. 2011; Spokas et al. 2012). Future improvements should focus on integrating additional field-based CO_2 flux measurements and refining the representation of microbial-driven carbon mineralization in the model framework (Blanco-Canqui 2017; Singh et al. 2012). Additionally, the long-term effects of biochar on soil carbon cycling need to be incorporated into the model to improve predictions over extended time scales (Woolf et al. 2018). Overall, this study confirms that the DLEM-Ag-Biochar model provides robust predictions of CO_2 emissions following biochar application, making it a valuable tool for assessing biochar's role in CSA. Future work should aim to refine biogeochemical feedback mechanisms and improve model calibration using long-term experimental data to enhance its predictive capabilities further (Lehmann et al. 2021; Ameloot et al. 2013).

4.2 Sensitivity of the DLEM-Ag-Biochar model

The sensitivity analysis shows coherent, rate-dependent responses across water, carbon, and nitrogen pathways in DLEM-Ag-Biochar. With increasing biochar, evaporation declined slightly (3098.8 to 3093.2 Mg ha^{-1}), and infiltration increased (6236.7 to 6242.9 Mg ha^{-1}), consistent with modification of pore-structure, reduced bulk density, and improved water retention (Laird et al. 2010; Atkinson et al. 2010; Jeffery et al. 2017; Major et al. 2012). Crop yield increased modestly (2543.2 to 2548.7 kg ha^{-1}), indicating limited short-term production gains. Soil C increased from 16.06 to 39.13 Mg ha^{-1}, confirming biochar's role in long-term carbon sequestration and relevance for climate mitigation (Lehmann and Joseph 2015; Woolf et al. 2010; Wang et al. 2016). In contrast, CO_2 emissions increased from 3836.2 to 4889.8 kg ha^{-1} and NEP declined from 2454.6 to 1412.1 kg ha^{-1}, suggesting enhanced microbial respiration or short-term priming effects following amendment, responses that vary across sites (Spokas et al. 2012; Kammann et al. 2017). CH_4 emissions decreased slightly (0.8848 to 0.8481 kg ha^{-1}), consistent with improved aeration and stimulation of methanotrophs (Atkinson et al. 2010; Major et al. 2012). Nitrogen cycling intensified with the application rate. The NH_4^+ pool increased from 6.15 to 13.49 kg ha^{-1}, nitrification increased from 3211.0 to 4483.6 kg ha^{-1}, and denitrification increased from 12.28 to 16.08 kg ha^{-1}. The concurrent rise in N_2O emissions (1.053 to 1.365 kg ha^{-1}) indicates that greater mineral N availability and redox-mediated transformations can offset expected mitigation, which varies with pH, cation exchange capacity, and electron acceptor dynamics (Glaser et al. 2002; Ding et al. 2016; Xu et al. 2014; Yao et al. 2012). Although many meta-analyses report reduced N_2O emissions via improved N retention and altered denitrification pathways, the direction and magnitude of responses remain site-specific and sensitive to application rate (Cayuela et al. 2014; Van Zwieten et al. 2014; Case et al. 2012; Spokas et al. 2012). Many studies report an average N_2O mitigation effect of biochar, including a synthesis that found an overall reduction across studies (Cayuela et al. 2014). However, increases in N_2O have also been documented and are often linked to conditions where nitrification-derived N_2O dominates, where biochar stimulates ammonia oxidizers and gross nitrification, or where the biochar-C to fertilizer-N balance favors greater N turnover (Sánchez-García et al. 2014; Prommer et al. 2014; Feng and Zhu 2017). The sensitivity analysis was conducted under the baseline cropping system and management settings used for this study, and the direction and magnitude of N_2O responses may differ under other crop rotations, fertilization regimes, and soil moisture and temperature conditions. This caveat is consistent with synthesis evidence that biochar impacts on N_2O vary with land use, soil properties, and environmental controls, and should not be interpreted as a universal increase across all cropping systems. Altogether, results indicate that higher biochar rates strengthen water infiltration and SOC sequestration and deliver small yield gains, but they also elevate CO_2 and N_2O and reduce NEP, revealing management trade-offs. Optimizing outcomes will require matching rate and particle size with soil texture and climate constraints, coupling biochar with nitrogen management to control mineral N accumulation and gaseous losses, and integrating irrigation scheduling to stabilize moisture regimes (Zhang et al. 2012b; Jeffery et al. 2017; Biederman and Harpole 2013). Long-term field validation is essential to quantify

persistence and to refine model parameterization for N transformations, priming dynamics, and biochar aging over time (Lehmann et al. 2011; Verheijen et al. 2010).

4.3 The potential of the DLEM-Ag-Biochar model

Recent advancements in agricultural modeling highlight the pressing need for comprehensive simulation frameworks tailored for innovative soil amendments such as biochar. Biochar has gained attention in recent decades for its agronomic benefits and carbon sequestration potential (Dokoohaki et al. 2018; Lehmann et al. 2011). Extensive research highlights the agronomic benefits of the complex interaction between the heterogeneous nature of the biochar and its ability to improve the soil health and crop yield (Huang et al. 2023; Kumar et al. 2025). Zhao et al (2022) emphasized the need of tools that help us to understand the effect of different types of biochar (e.g., different values of feedstock, pyrolysis temperature, surface area, ash content, and C/H/O/N content) on all kinds of soil types (e.g., different values of texture, dry bulk density, moisture content, organic matter content, and porosity) under various environmental situations (e.g., temperature, rainfall, evaporation, crops, and management measures). In response, this study presents the development and application of DLEM-Ag-Biochar, a novel computational framework for simulating and predicting the multidimensional impacts of biochar amendments across heterogeneous agricultural ecosystems.

The DLEM-Ag-Biochar offers practical applications that extend beyond theoretical evaluations. It can address the critical gap in current research by transforming limited short-term experimental datasets into comprehensive long-term projections, as highlighted by the validation results. By accurately capturing complex soil–plant-atmospheric dynamics, the model avoids the excessive costs and time constraints typically associated with traditional field experiments. Delgado et al. (2019) and Zhai et al. (2020) showed that computational frameworks can expedite the optimization of agricultural practices, supporting advancements in sustainable farming systems. A key strength of ecosystem models such as DLEM-Ag-Biochar is their ability to function as a virtual experimental laboratory. Researchers can efficiently assess a wide array of variables including varied biochar application rates, amendment compositions, and environmental conditions to identify optimal strategies tailored to specific agricultural contexts. For instance, the model can perform simulation of decades of crop cycles within hours, while incorporating dynamic factors such as climate variability, soil properties, and diverse management practices. This capability allows researchers to narrow down promising configurations before undertaking resource-intensive field trials.

Critically, this framework can be used as a decision-support tool to recommend region-specific biochar strategies. This is achieved by systematically linking (i) regional climate and soil constraints (e.g., texture, baseline soil organic carbon (SOC), pH, and moisture regime) with (ii) measurable biochar properties determined by feedstock and pyrolysis conditions, and (iii) conducting scenario simulations across a feasible range of application rates to quantify trade-offs among crop yield, SOC accrual, and GHG outcomes. This approach follows established guidance that application rate and biochar type should be tailored to local soil and management conditions rather than using blanket recommendations (American Farmland Trust 2026) and aligns with the conclusion that locally specific decision support is necessary because biochar outcomes are heterogeneous and depend on feedstock and production choices (International Biochar Initiative 2026; Lehmann et al. 2021). Biochar selection can be operationalized within the model through standardized, property-based classification, enabling precise matching of biochar characteristics to local soil deficiencies or goals. Recent evidence emphasizes the geographically varying responses to biochar and the strong role of application rate and nitrogen management in driving this spatial heterogeneity (Chen et al. 2024; Xu et al. 2025), a complexity the DLEM-Ag-Biochar model is designed to unravel.

4.4 Knowledge gaps and future research opportunities

This study sets the basis for a mechanistic and system-level assessment of biochar effects on soils and crops and the potential trade-offs. We envision that the biochar model will shed light on critical questions and generate hypotheses for experimental research. The biochar model is still a nascent technology and has great potential to assist agronomists, soil scientists, economists, and policymakers in designing sustainable and profitable biochar-based major cropping systems. Moreover, most sites in this study conducted short-term experiments focused on individual variables, such as crop yield, SOC, and GHG emissions. Samples were also uneven across modeled variables and stratification conditions, introducing uncertainty to subgroup evaluation and extrapolation. For example, yield observations in the arid zone (n = 36) were fewer than those in the tropical zone (n = 82). Similar imbalances occurred for SOC and CO_2, including limited temperate SOC observations (n = 10) and sparse CO_2 data in tropical (n = 4) and arid (n = 8) zones compared with cold regions (n = 66). Therefore, performance metrics for data-sparse strata should be interpreted more cautiously, and future calibration and validation should

prioritize expanding long-term, co-located measurements of yield, SOC, and GHG fluxes in underrepresented environments to better constrain parameters and improve model generalizability. Furthermore, while this study focused on yield, SOC and CO_2 flux due to the availability of consistent multi-year datasets for global benchmarking, incorporating non-CO_2 greenhouse gases (N_2O and CH_4) is a critical next step. A priority for future work is to test whether the rate response of N_2O (and other N transformation fluxes) is consistent across contrasting cropping systems and climates by expanding long-term, co-located observations and running multi-factor scenario ensembles. Such datasets are needed to better constrain how biochar alters the balance between nitrification-derived and denitrification-derived N_2O under crop-specific N demand and moisture regimes. These trace gases are essential for a comprehensive evaluation of Climate-Smart Agriculture (CSA) objectives, as they represent potent climate forcing agents that significantly influence the net mitigation potential of agricultural systems (Paustian et al. 2016; Smith 2016). Although SOC changes indicate carbon sequestration, coupling these stocks with process-level CO_2 efflux and trace gas fluxes provides a more robust constraint on the total ecosystem carbon and greenhouse gas balance (Woolf et al. 2010).

The reliability of process-based models like DLEM-Ag-Biochar fundamentally depends on high-quality, long-term empirical data to validate and refine model assumptions. This study focused on biochar in maize, wheat, and soybean systems due to sufficient multi-variable field data and the model's established calibration for these upland crops. Flooded rice systems were excluded because they require distinct representations of paddy hydrology and methane production, which are relatively simplied in the current module's scope; and meanwhile the available biochar dataset for rice was also inadequate for robust parameterization. Also, expanding calibration and validation efforts using extended field trials is critical to capture a broader range of ecosystem services (e.g., yield, soil chemistry, nutrient fluxes) as the data become available. In summary, these data will be essential for achieving our specific model development goals: (1) finalizing and expanding calibration across diverse environments, cropping systems, and biochar types, (2) creating a user-accessible database for calibrated biochar parameters to facilitate systematic analysis, (3) implementing and enhancing mechanistic modules, most pivotally by explicitly distinguishing between fresh and aged biochar properties to dynamically represent the aging effects, as well as by incorporating processes such as biochar impacts on microbial and root dynamics, and (4) extending the module to simulate N_2O and CH_4 fluxes to align model outputs with the full suite of CSA mitigation targets. We also recommend that field scientists keep detailed site-specific information, along with a calendar of crop management practices, to ensure these studies can more effectively support modeling efforts.

5 Conclusion

In this study, we developed and tested a new biochar model. Our findings highlight the effectiveness of biochar as a CSA strategy, emphasizing the module's role in simulating crop yield, soil carbon storage, and GHG emissions. The DLEM-Ag-Biochar model demonstrated robust predictive capability across various environmental conditions, but performance declines under extreme environmental conditions, indicating the need for targeted refinement. Simulations show that biochar's impact varies by soil type, climate, and management practices, necessitating further validation through long-term field trials and applications. Future work should focus on integrating microbial interactions with soil physicochemical properties to optimize biochar use for sustainable agriculture and climate mitigation. This study provides a foundation for improved biochar modeling and implementation.

Supplementary Information

The online version contains supplementary material available at https://doi.org/10.1007/s42773-026-00609-9.

Additional file1 (DOCX 504 KB)

Acknowledgements

We gratefully acknowledge the financial support provided by Alfred P. Sloan Foundation (grant no. G-2019-12468) and the US National Science Foundation (grant no. 2045235/2327138). Yawen Huang acknowledges funding support from the National Natural Science Foundation of China (42507653), and the Start-up Foundation for Introducing Talent of Nanjing Agricultural University (no. 030/804188).

Author contributions

Wei Ren: conceptualization, funding acquisition, investigation, methodology, project administration, supervision, validation, visualization, writing—original draft, writing—review and editing. Yogesh Kumar: data curation, formal analysis, methodology, resources, validation, visualization, writing—original draft, writing—review and editing. Yawen Huang: methodology, funding acquisition, validation, visualization, writing—original draft, writing—review and editing. All authors read and approved the final manuscript.

Funding

This work was supported by grants from the Alfred P. Sloan Foundation (grant no. G-2019-12468) and the US National Science Foundation (grant no. 2045235/2327138). Yawen Huang acknowledges funding support from the National Natural Science Foundation of China (42507653) and the Start-up Foundation for Introducing Talent of Nanjing Agricultural University (no. 030/804188).

Data availability
The datasets used or analyzed during the current study are available from the corresponding author upon reasonable request. A standalone user interface and documentation are planned for future release.

Declarations

Ethics approval and consent to participate
Not applicable.

Competing interests
The authors declare no conflicts of interest.

Author details
[1]Department of Natural Resources and the Environment, University of Connecticut, Storrs, CT 06269, USA. [2]Key Laboratory of Low-Carbon and Green Agriculture in Southeastern China, Ministry of Agriculture and Rural Affairs, College of Resources and Environmental Sciences, Nanjing Agricultural University, Nanjing 210095, Jiangsu, China.

Received: 4 November 2025 Revised: 16 February 2026 Accepted: 13 March 2026
Published online: 24 April 2026

References

Ameloot N, Graber ER, Verheijen FGA, De Neve S (2013) Interactions between biochar stability and soil organisms: review and research needs. Eur J Soil Sci 64(4):379–390. https://doi.org/10.1111/ejss.12064
American Farmland Trust (2026). Biochar in agriculture toolkit. Farmland Information Center. https://farmlandinfo.org/biochar-in-agriculture-toolkit/. Accessed 1 Feb 2026.
Archontoulis SV, Huber I, Miguez FE, Thorburn PJ, Rogovska N, Laird DA (2016) A model for mechanistic and system assessments of biochar effects on soils and crops and trade-offs. GCB Bioenergy 8(6):1028–1045. https://doi.org/10.1111/gcbb.12314
Atkinson CJ, Fitzgerald JD, Hipps NA (2010) Potential mechanisms for achieving agricultural benefits from biochar application to temperate soils: a review. Plant Soil 337(1–2):1–18. https://doi.org/10.1007/s11104-010-0464-5
Banger K, Tian H, Tao B, Lu C, Ren W, Yang J (2015) Magnitude, spatiotemporal patterns, and controls for soil organic carbon stocks in India during 1901–2010. Soil Sci Soc Am J 79(3):864–875
Biederman LA, Harpole WS (2013) Biochar and its effects on plant productivity and nutrient cycling: a meta-analysis. GCB Bioenergy 5(2):202–214. https://doi.org/10.1111/gcbb.12037
Blanco-Canqui H (2017) Biochar and soil physical properties. Soil Sci Soc Am J 81(4):687–711. https://doi.org/10.2136/sssaj2017.01.0017
Case SDC, McNamara NP, Reay DS, Whitaker J (2012) The effect of biochar addition on N2O and CO2 emissions from a sandy loam soil: the role of soil aeration. Soil Biol Biochem 51:125–134. https://doi.org/10.1016/j.soilbio.2012.03.017
Cayuela ML, van Zwieten L, Singh BP, Jeffery S, Roig A, Sanchez-Monedero MA (2014) Biochar's role in mitigating soil nitrous oxide emissions: a review and meta-analysis. Agric Ecosyst Environ 191:5–16. https://doi.org/10.1016/j.agee.2013.10.009
Chen M, Ran H, Sommer SG, Liu Y, Wang G, Zhu K (2024) The spatiotemporal heterogeneity of fertosphere hotspots impacted by biochar addition and the implications for NH3 and N2O emissions. Chemosphere 355:141769. https://doi.org/10.1016/j.chemosphere.2024.141769
Cheng CH, Lehmann J, Engelhard MH (2008) Natural oxidation of black carbon in soils: changes in molecular form and surface charge along a climosequence. Geochim Cosmochim Acta 72(6):1598–1610. https://doi.org/10.1016/j.gca.2008.01.010
Crane-Droesch A, Abiven S, Jeffery S, Torn MS (2013) Heterogeneous global crop yield response to biochar: a meta-regression analysis. Environ Res Lett 8(4):044049. https://doi.org/10.1088/1748-9326/8/4/044049
Danalatos NG, Kosmas CS, Driessen PM, Yassoglou N (1994) The change in the specific leaf area of maize grown under Mediterranean conditions. Agronomie 14(7):433–443. https://doi.org/10.1051/agro:19940702
Delgado JA, Short NM Jr, Roberts DP, Vandenberg B (2019) Big data analysis for sustainable agriculture on a geospatial cloud framework. Front Sustain Food Syst 3:54. https://doi.org/10.3389/fsufs.2019.00054
Denef K, Six J, Bossuyt H, Frey SD, Elliott ET, Merckx R, Paustian K (2001) Influence of dry–wet cycles on the interrelationship between aggregate, particulate organic matter, and microbial community dynamics. Soil Biol Biochem 33(12–13):1599–1611. https://doi.org/10.1016/S0038-0717(01)00076-1
Ding Y, Liu Y, Liu S, Li Z, Tan X, Huang X, Zheng B (2016) Biochar to improve soil fertility: a review. Agron Sustain Dev 36(2):Article 36. https://doi.org/10.1007/s13593-016-0372-z
Dokoohaki H, Miguez FE, Archontoulis SV, Laird DA (2018) Use of inverse modelling and Bayesian optimization for investigating the effect of biochar on soil hydrological properties. Agric Water Manag 208:268–274. https://doi.org/10.1016/j.agwat.2018.06.034
Drewniak B, Song J, Prell J, Kotamarthi VR, Jacob R (2013) Modeling agriculture in the Community Land Model. Geosci Model Dev 6(2):495–515. https://doi.org/10.5194/gmd-6-495-2013
Feng Z, Zhu L (2017) Impact of biochar on soil N2O emissions under different biochar-carbon/fertilizer-nitrogen ratios at a constant moisture condition on a silt loam soil. Sci Total Environ 584–585:776–782. https://doi.org/10.1016/j.scitotenv.2017.01.115
Gai X, Wang H, Liu J, Zhai L, Liu S, Ren T, Liu H (2014) Effects of feedstock and pyrolysis temperature on biochar adsorption of ammonium and nitrate. PLoS ONE 9(12):e113888. https://doi.org/10.1371/journal.pone.0113888
Glaser B, Lehmann J, Zech W (2002) Ameliorating physical and chemical properties of highly weathered soils in the tropics with charcoal: a review. Biol Fertil Soils 35(4):219–230. https://doi.org/10.1007/s00374-002-0466-4
Gurwick NP, Moore LA, Kelly C, Elias P (2013) A systematic review of biochar research, with a focus on its stability in situ and its promise as a climate mitigation strategy. PLoS ONE 8(9):e75932. https://doi.org/10.1371/journal.pone.0075932
Haghnegahdar A, Razavi S (2017) Insights into sensitivity analysis of Earth and environmental systems models: on the impact of parameter perturbation scale. Environ Model Softw 95:115–131. https://doi.org/10.1016/j.envsoft.2017.03.031
Hamby DM (1994) A review of techniques for parameter sensitivity analysis of environmental models. Environ Monit Assess 32(2):135–154. https://doi.org/10.1007/BF00547132
Han M, Zhao Q, Wang X, Wang YP, Ciais P, Zhang H, Goll DS, Zhu L, Zhao Z, Guo Z, Wang C, Zhuang W, Wu F, Li W (2024) Modeling biochar effects on soil organic carbon on croplands in a microbial decomposition model (MIMICS-BC_v1. 0). Geoscientific Model Dev 17(12):4871–4890
Hassink J (1997) The capacity of soils to preserve organic C and N by their association with clay and silt particles. Plant Soil 191(1):77–87. https://doi.org/10.1023/A:1004213929699
Huang Y, Ren W, Grove J1, Poffenbarger H, Jacobsen K, Tao B, Zhu X, McNear D (2020) Assessing synergistic effects of no-tillage and cover crops on soil carbon dynamics in a long-term maize cropping system under climate change. Agric For Meteorol 291:108090. https://doi.org/10.1016/j.agrformet.2020.108090
Huang Y, Ren W, Lindsey LE, Wang L, Hui D, Tao B, Jacinthe PA, Tian H (2024) No-tillage farming enhances widespread nitrate leaching in the US Midwest. Environ. Res. Lett. 19(10): 104062
Huang Y, Tao B, Zhu X, Yang Y, Liang L, Wang L, Jacinthe P, Tian H, Ren W† (2021) Conservation tillage increases corn and soybean water productivity across the Ohio River Basin. Agric Water Manag 254:106962 https://doi.org/10.1016/j.agwat.2021.106962
Huang Y, Tao B, Yang Y, Zhu X, Yang XJ, Grove J, Ren W (2022) Modeling crop yield and greenhouse gas emissions in Kentucky no-tillage corn and soybean cropping systems: 1980–2018. Agric Syst 197:103355. https://doi.org/10.1016/j.agsy.2021.103355
Huang Y, Tao B, Lal R, Lorenz K, Jacinthe PA, Shrestha RK, Bai X, Singh MP, Lindsey LE, Ren W (2023) A global synthesis of biochar's sustainability in climate-smart agriculture - evidence from field and laboratory experiments. Renew Sustain Energy Rev 172:113042. https://doi.org/10.1016/j.rser.2022.113042
International Biochar Initiative (2026) Biochar classification tool. https://biochar-international.org/resources/biochar-classification-tool/. Accessed 1 Feb 2026

Ippolito JA, Cui L, Kammann C, Wrage-Mönnig N, Estavillo JM, Fuertes-Mendizabal T, Cayuela ML, Sigua G, Novak J, Spokas K, Borchard N (2020) Feedstock choice, pyrolysis temperature and type influence biochar characteristics: a comprehensive meta-data analysis review. Biochar 2(4):421–438

Jamieson PD, Porter JR, Wilson DR (1991) A test of the computer simulation model ARCWHEAT1 on wheat crops grown in New Zealand. Field Crops Res 27(4):337–350

Jeffery S, Verheijen FGA, van der Velde M, Bastos AC (2011) A quantitative review of the effects of biochar application to soils on crop productivity using meta-analysis. Agric Ecosyst Environ 144(1):175–187. https://doi.org/10.1016/j.agee.2011.08.015

Jeffery S, Abalos D, Prodana M, Bastos AC, van Groenigen JW, Hungate BA, Verheijen F (2017) Biochar boosts tropical but not temperate crop yields. Environ Res Lett 12(5):053001. https://doi.org/10.1088/1748-9326/aa67bd

Jones DL, Rousk J, Edwards-Jones G, DeLuca TH, Murphy DV (2012) Biochar-mediated changes in soil quality and plant growth in a three year field trial. Soil Biol Biochem 45:113–124

Joseph SD, Camps-Arbestain M, Lin Y, Munroe P, Chia CH, Hook J, van Zwieten L, Kimber S, Cowie A, Singh BP, Lehmann J, Foidl N, Smernik RJ, Amonette JE (2010) An investigation into the reactions of biochar in soil. Aust J Soil Res 48(7):501–515. https://doi.org/10.1071/SR10009

Kammann CI, Schmidt HP, Messerschmidt N, Linsel S, Steffens D, Müller C, Koyro HW, Conte P, Joseph S (2015) Plant growth improvement mediated by nitrate capture in co-composted biochar. Sci Rep 5:Article 11080. https://doi.org/10.1038/srep11080

Kammann C, Ippolito J, Hagemann N, Borchard N, Cayuela ML, Estavillo JM, Fuertes-Mendizabal T, Jeffery S, Kern J, Novak J, Rasse DP, Saarnio S, Schmidt HP, Spokas K, Wrage-Mönnig N (2017) Biochar as a tool to reduce the agricultural greenhouse-gas burden - knowns, unknowns and future research needs. J Environ Eng Landsc Manag 25(2):114–139. https://doi.org/10.3846/16486897.2017.1319375

Kaur N, Hui D, Kieffer C, Ren W (2023) How much is soil nitrous oxide emission reduced with biochar application? An evaluation of meta-analyses. GCB Bioenergy. https://doi.org/10.1111/gcbb.13003

Kravchenko AN, Negassa WC, Guber AK, Rivers ML (2015) Protection of soil carbon within macro-aggregates depends on intra-aggregate pore characteristics. Sci Rep 5:16261. https://doi.org/10.1038/srep16261

Kumar Y, Ren W, Tao H, Tao B, Lindsey LE (2025) Impact of biochar amendment on soil microbial biomass carbon enhancement under field experiments: a meta-analysis. Biochar 7:Article 2. https://doi.org/10.1007/s42773-024-00391-6

Kuzyakov Y, Gavrichkova O (2010) Time lag between photosynthesis and carbon dioxide efflux from soil: A review of mechanisms and controls. Glob Change Biol 16(12):3386–3406. https://doi.org/10.1111/j.1365-2486.2010.02179.x

Laird DA, Fleming P, Davis DD, Horton R, Wang B, Karlen DL (2010) Impact of biochar amendments on the quality of a typical Midwestern agricultural soil. Geoderma 158(3–4):443–449. https://doi.org/10.1016/j.geoderma.2010.05.013

Lehmann J, Gaunt J, Rondon M (2006) Bio-char sequestration in terrestrial ecosystems: a review. Mitig Adapt Strateg Glob Change 11(2):403–427. https://doi.org/10.1007/s11027-005-9006-5

Lehmann J, Rillig MC, Thies J, Masiello CA, Hockaday WC, Crowley D (2011) Biochar effects on soil biota: a review. Soil Biol Biochem 43(9):1812–1836. https://doi.org/10.1016/j.soilbio.2011.04.022

Lehmann J, Hansel CM, Kaiser C, Kleber M, Maher K, Manzoni S, Nunan N, Reichstein M, Schimel JP, Torn MS, Wieder WR, Kögel-Knabner I (2020) Persistence of soil organic carbon caused by functional complexity. Nat Geosci 13(8):529–534. https://doi.org/10.1038/s41561-020-0612-3

Lehmann J, Cowie A, Masiello CA, Kammann C, Woolf D, Amonette JE, Cayuela ML, Camps-Arbestain M, Whitman T (2021) Biochar in climate change mitigation. Nat Geosci 14(12):883–892. https://doi.org/10.1038/s41561-021-00852-8

Lehmann J, Joseph S (Eds) (2015) Biochar for environmental management: Science, technology and implementation, 2nd edn. Routledge, London. https://doi.org/10.4324/9780203762264

Lenhart T, Eckhardt K, Fohrer N, Frede H-G (2002) Comparison of two different approaches of sensitivity analysis. Phys Chem Earth Parts a/b/c 27(9–10):645–654. https://doi.org/10.1016/S1474-7065(02)00049-9

Liu X, Zhang A, Ji C, Joseph S, Bian R, Li L, Pan G, Paz-Ferreiro J (2013) Biochar's effect on crop productivity and the dependence on experimental conditions: a meta-analysis of literature data. Plant Soil 373(1–2):583–594. https://doi.org/10.1007/s11104-013-1806-x

Lu X, Ju W, Li J, Croft H, Chen JM, Luo Y, Yu H, Hu H (2020) Maximum carboxylation rate estimation with chlorophyll content as a proxy of rubisco content. J Geophys Res: Biogeosciences 125(8): e2020JG005748

Luo Z, Wang E, Sun OJ (2010) Soil carbon change and its responses to agricultural practices in Australian agro-ecosystems: a review and synthesis. Geoderma 155(3–4):211–223. https://doi.org/10.1016/j.geoderma.2009.12.012

Major J, Rondon M, Molina D, Riha SJ, Lehmann J (2010) Maize yield and nutrition during 4 years after biochar application to a Colombian savanna Oxisol. Plant Soil 333:117–128. https://doi.org/10.1007/s11104-010-0327-0

Major J, Rondon M, Molina D, Riha SJ, Lehmann J (2012) Nutrient leaching in a Colombian savanna Oxisol amended with biochar. J Environ Qual 41(4):1076–1086. https://doi.org/10.2134/jeq2011.0128

Nelson PN, Su N (2010) Soil pH buffering capacity: a descriptive function and its application to some acidic tropical soils. Soil Res 48(3):201–207

Parton WJ, Ojima DS, Cole CV, Schimel DS (1994) A general model for soil organic matter dynamics: sensitivity to litter chemistry, texture and management. Quantitative Model Soil Forming Processes 39:147–167

Paustian K, Lehmann J, Ogle S, Reay D, Robertson GP, Smith P (2016) Climate-smart soils. Nature 532(7597):49–57. https://doi.org/10.1038/nature17174

Pianosi F, Beven K, Freer J, Hall JW, Rougier J, Stephenson DB, Wagener T (2016) Sensitivity analysis of environmental models: a systematic review with practical workflow. Environ Model Softw 79:214–232. https://doi.org/10.1016/j.envsoft.2016.02.008

Powlson DS, Whitmore AP, Goulding KWT (2011) Soil carbon sequestration to mitigate climate change: a critical re-examination to identify the true and the false. Eur J Soil Sci 62(1):42–55. https://doi.org/10.1111/j.1365-2389.2010.01342.x

Prommer J, Wanek W, Hofhansl F, Trojan D, Offre P, Urich T, Schleper C, Sassmann S, Kitzler B, Soja G (2014) Biochar decelerates soil organic nitrogen cycling but stimulates soil nitrification in a temperate arable field trial. PLoS ONE 9(1):e86388. https://doi.org/10.1371/journal.pone.0086388

Pulcher A et al (2022) Biochar and its effects on soil organic carbon: a review of experimental and modelling findings. SOIL 8:199–226. https://doi.org/10.5194/soil-8-199-2022

Qian X, Liu L, Chen X, Zarco-Tejada PJ (2021) Assessment of satellite chlorophyll-based leaf maximum carboxylation rate (Vcmax) using flux observations at crop and grass sites. IEEE J Sel Top Appl Earth Obs Remote Sens 14:5352–5360. https://doi.org/10.1109/JSTARS.2021.3081704

Quebbeman JA, Ramirez JA (2016) Optimal allocation of leaf-level nitrogen: implications for covariation of Vcmax and Jmax and photosynthetic downregulation. J Geophys Res Biogeosci 121(9):2464–2475. https://doi.org/10.1002/2016JG003473

Ren W (2019) Towards an integrated agroecosystem modeling approach for climate-smart agricultural management. In Bridging among disciplines by synthesizing soil and plant processes, Vol. 8, American Society of Agronomy, Crop Science Society of America, and Soil Science Society of America Books, USA, pp 127–144

Ren W, Tian H, Tao B, Chappelka A, Sun G, Lu C, Liu M, Chen G, Xu X (2011) Impacts of tropospheric ozone and climate change on net primary productivity and net carbon exchange of China's forest ecosystems. Global Ecol Biogeogr 20(3):391–406

Ren W, Tian H, Tao B, Huang Y, Pan S (2012) China's crop productivity and soil carbon storage as influenced by multifactor global change. Glob Change Biol 18(9):2945–2957. https://doi.org/10.1111/j.1365-2486.2012.02741.x

Ren W, Tian H, Cai W, Lohrenz SE, Hopkinson CS, Huang W, Yang J, Tao B, Pan S, He R (2016) Century-long increasing trend and variability of dissolved organic carbon export from the Mississippi River basin driven by natural and anthropogenic forcing. Glob Biogeochem Cycles 30(9):1288–1299. https://doi.org/10.1002/2016GB005395

Ren W, Banger K, Tao B, Yang J, Huang Y, Tian H (2020) Global pattern and change of cropland soil organic carbon during 1901–2010: roles of

climate, atmospheric chemistry, land use and management. Geogr Sustain 1(1):59–69. https://doi.org/10.1016/j.geosus.2020.03.001
Rondon MA, Lehmann J, Ramirez J, Hurtado M (2007) Biological nitrogen fixation by common beans (*Phaseolus vulgaris* L.) increases with biochar additions. Biol Fertil Soils 43(6):699–708. https://doi.org/10.1007/s00374-006-0152-z
Saltelli A, Tarantola S, Campolongo F, Ratto M (2004) Sensitivity analysis in practice: a guide to assessing scientific models. John Wiley & Sons. https://doi.org/10.1002/0470870958
Saltelli A, Ratto M, Andres T, Campolongo F, Cariboni J, Gatelli D, Saisana M, Tarantola S (2008) Global sensitivity analysis: The primer. John Wiley & Sons. https://doi.org/10.1002/9780470725184
Sánchez-García M, Roig A, Sánchez-Monedero MA, Cayuela ML (2014) Biochar increases soil N2O emissions produced by nitrification-mediated pathways. Front Environ Sci 2:25. https://doi.org/10.3389/fenvs.2014.00025
Schimel JP, Bilbrough C, Welker JM (2004) Increased snow depth affects microbial activity and nitrogen mineralization in two Arctic tundra communities. Soil Biol Biochem 36(2):217–227. https://doi.org/10.1016/j.soilbio.2003.09.008
Schmidt H-P, Hagemann N, Draper K, Kammann C (2021) Biochar in agriculture: a systematic review of 26 global meta-analyses. GCB Bioenergy 13(11):1708–1730. https://doi.org/10.1111/gcbb.12889
Seybold CA, Grossman RB (2006) Prediction of effective cation exchange capacity in low pH soils. Soil Sci 171(1):3–12
Shrestha RK, Jacinthe P-A, Lal R, Lorenz K, Singh MP, Demyan SM, Ren W, Lindsey LE (2023) Biochar as a negative emission technology: a synthesis of field research on greenhouse gas emissions. J Environ Qual 52(4):769–798. https://doi.org/10.1002/jeq2.20475
Singh BP, Cowie AL, Smernik RJ (2012) Biochar carbon stability in a clayey soil as a function of feedstock and pyrolysis temperature. Environ Sci Technol 46(21):11770–11778. https://doi.org/10.1021/es302545b
Six J, Conant RT, Paul EA, Paustian K (2002) Stabilization mechanisms of soil organic matter: implications for C-saturation of soils. Plant Soil 241(2):155–176. https://doi.org/10.1023/A:1016125726789
Smith P (2004) How long before a change in soil organic carbon can be detected? Glob Change Biol 10(11):1878–1883
Smith P (2016) Soil carbon sequestration and biochar as negative emission technologies. Glob Change Biol 22(3):1315–1324. https://doi.org/10.1111/gcb.13178
Smith P, Martino D, Cai Z, Gwary D, Janzen H, Kumar P, McCarl B, Ogle S, O'Mara F, Rice C, Scholes B, Sirotenko O, Howden M, McAllister T, Pan G, Romanenkov V, Schneider U, Towprayoon S, Wattenbach M, Smith J (2008) Greenhouse gas mitigation in agriculture. Philos Trans R Soc Lond B Biol Sci 363(1492):789–813. https://doi.org/10.1098/rstb.2007.2184
Spokas KA, Cantrell KB, Novak JM, Archer DW, Ippolito JA, Collins HP, Boateng AA, Lima IM, Lamb MC, McAloon AJ, Lentz RD, Nichols KA (2012) Biochar: a synthesis of its agronomic impact beyond carbon sequestration. J Environ Qual 41(4):973–989. https://doi.org/10.2134/jeq2011.0069
Sun H, Lu H, Chu L, Shao H, Shi W (2017) Biochar applied with appropriate rates can reduce N leaching, keep N retention and not increase NH_3 volatilization in a coastal saline soil. Sci Total Environ 575:820–825. https://doi.org/10.1016/j.scitotenv.2016.09.137
Tardieu F, Granier C, Müller B (1999) Modelling leaf expansion in a fluctuating environment: are changes in specific leaf area a consequence of changes in expansion rate? New Phytol 143(1):33–43. https://doi.org/10.1046/j.1469-8137.1999.00433.x
Thangarajan R, Bolan NS, Tian G, Naidu R, Kunhikrishnan A (2013) Role of organic amendment application on greenhouse gas emission from soil. Sci Total Environ 465:72–96. https://doi.org/10.1016/j.scitotenv.2013.01.031
Tian H, Xu X, Liu M, Ren W, Zhang C, Chen G, Lu C (2010) Spatial and temporal patterns of CH_4 and N_2O fluxes in terrestrial ecosystems of North America during 1979–2008: application of a global biogeochemistry model. Biogeosciences 7(9):2673–2694
Tian H, Chen G, Zhang C, Liu M, Sun G, Chappelka A, Ren W, Xu X, Lu C, Pan S, Chen H, Hui D, McNulty S, Lockaby G, Vance E (2012) Century-scale responses of ecosystem carbon storage and flux to multiple environmental changes in the southern United States. Ecosystems 15(4):674–694
Tian H, Chen G, Lu C, Xu X, Hayes DJ, Ren W, Pan S, Huntzinger DN, Wofsy SC (2015) North American terrestrial CO2 uptake largely offset by CH4 and N2O emissions: toward a full accounting of the greenhouse gas budget. Clim Change 129(3):413–426
Tiemann LK, Grandy AS, Atkinson EE, Marin-Spiotta E, McDaniel MD (2015) Crop rotational diversity enhances belowground communities and functions in an agroecosystem. Ecol Lett 18(8):761–771. https://doi.org/10.1111/ele.12453
Van Zwieten L, Singh BP, Kimber SWL, Murphy DV, Macdonald LM, Rust J, Morris S (2014) An incubation study investigating the mechanisms that impact N2O flux from soil following biochar application. Agric Ecosyst Environ 191:53–62. https://doi.org/10.1016/j.agee.2014.02.030
Ventura M, Alberti G, Viger M, Jenkins JR, Girardin C, Baronti S, Zaldei A, Taylor G, Rumpel C, Miglietta F, Tonon G (2015) Biochar mineralization and priming effect on SOM decomposition in two European short rotation coppices. GCB Bioenergy 7(5):1150–1160
Verheijen F, Jeffery S, Bastos AC, Van der Velde M, Diafas I (2010) Biochar application to soils. A critical scientific review of effects on soil properties, processes, and functions. EUR 24099(162):2183–2207. https://doi.org/10.2788/472
Wang Y, Huang Y, Ren W (2025) Adaptive strategies for reducing yield-scaled nitrate leaching in the US Midwest. Earth's Future 13(10) e2025EF006410
Wang J, Xiong Z, Kuzyakov Y (2016) Biochar stability in soil: meta-analysis of decomposition and priming effects. GCB Bioenergy 8(3):512–523. https://doi.org/10.1111/gcbb.12266
Wang D, Li C, Parikh SJ, Scow KM (2019) Impact of biochar on water retention of two agricultural soils: a multi-scale analysis. Geoderma 340:185–191. https://doi.org/10.1016/j.geoderma.2019.01.012
Wang X, Lu P, Yang P, Ren S (2021) Effects of fertilizer and biochar applications on the relationship among soil moisture, temperature, and N2O emissions in farmland. PeerJ 9:e11674
Weng Z, Van Zwieten L, Singh BP, Tavakkoli E, Joseph S, Macdonald LM, Cowie AL (2017) Biochar built soil carbon over a decade by stabilizing rhizodeposits. Nat Clim Change 7(5):371–376. https://doi.org/10.1038/nclimate3276
Woolf D, Amonette JE, Street-Perrott FA, Lehmann J, Joseph S (2010) Sustainable biochar to mitigate global climate change. Nat Commun 1:Article 56. https://doi.org/10.1038/ncomms1053
Woolf D, Lehmann J, Cowie A, Cayuela ML, Whitman T, Sohi S (2018) Biochar for climate change mitigation. Soil Clim 219:248
Xu H-J, Wang X-H, Li H, Yao H-Y, Su J-Q, Zhu Y-G (2014) Biochar impacts soil microbial community composition and nitrogen cycling in an acidic soil planted with rape. Environ Sci Technol 48(16):9391–9399. https://doi.org/10.1021/es5021058
Xu N, Tan G, Wang H, Gai X (2016) Effect of biochar additions to soil on nitrogen leaching, microbial biomass and bacterial community structure. Eur J Soil Biol 74:1–8. https://doi.org/10.1016/j.ejsobi.2016.02.004
Xu Z, Zhou R, Xu G (2025) Global analysis on potential effects of biochar on crop yields and soil quality. Soil Ecol Lett 7(1):Article 240267. https://doi.org/10.1007/s42832-024-0267-x
Yao Y, Gao B, Zhang M, Inyang M, Zimmerman AR (2012) Effect of biochar amendment on sorption and leaching of nitrate, ammonium, and phosphate in a sandy soil. Chemosphere 89(11):1467–1471. https://doi.org/10.1016/j.chemosphere.2012.06.002
You Y, Tian H, Pan S, Shi H, Bian Z, Gurgel A, Huang Y, Kicklighterf D, Liang X, Lu C, Melillo J, Miao R, Pan N, Reilly J, Ren W, Xu R, Yang J, Yu Q, Zhang J (2022) Incorporating dynamic crop growth processes and management practices into a terrestrial biosphere model for simulating crop production in the United States: toward a unified modeling framework. Agric for Meteorol. https://doi.org/10.1016/j.agrformet.2022.109144.
Zhai Z, Martínez JF, Beltran V, Martínez NL (2020) Decision support systems for agriculture 4.0: survey and challenges. Comput Electron Agric 170:105256. https://doi.org/10.1016/j.compag.2020.105256
Zhang A, Bian R, Pan G, Cui L, Hussain Q, Li L, Zheng J, Zheng J, Zhang X, Han X, Yu X (2012a) Effects of biochar amendment on soil quality, crop yield and greenhouse gas emission in a Chinese rice paddy: a field study of 2 consecutive rice growing cycles. Field Crops Res 127:153–160. https://doi.org/10.1016/j.fcr.2011.11.020
Zhang A, Liu Y, Pan G, Hussain Q, Li L, Zheng J, Zhang X (2012b) Effect of biochar amendment on maize yield and greenhouse gas emissions from a

soil organic carbon poor calcareous loamy soil from Central China Plain. Plant Soil 351:263–275. https://doi.org/10.1007/s11104-011-0957-x

Zhang J, Tian H, Yang J, Pan S (2018) Improving representation of crop growth and yield in the dynamic land ecosystem model and its application to China. J Adv Model Earth Syst 10(7):1680–1707

Zhao Y, Li Y, Yang F (2022) A state-of-the-art review on modeling the biochar effect: guidelines for beginners. Sci Total Environ 802:149861. https://doi.org/10.1016/j.scitotenv.2021.149861

Zimmerman AR, Gao B, Ahn M-Y (2011) Positive and negative carbon mineralization priming effects among a variety of biochar-amended soils. Soil Biol Biochem 43(6):1169–1179. https://doi.org/10.1016/j.soilbio.2011.02.005